

Switch EMA: A Free Lunch for Better Flatness and Sharpness

Siyuan Li^{*123} Zicheng Liu^{*13} Juanxi Tian^{*1} Ge Wang^{*13} Zedong Wang¹ Weiyang Jin¹ Di Wu¹³
Cheng Tan¹³ Tao Lin¹ Yang Liu² Baigui Sun² Stan Z. Li¹

Abstract

Exponential Moving Average (EMA) is a widely used weight averaging (WA) regularization to learn flat optima for better generalizations without extra cost in deep neural network (DNN) optimization. Despite achieving better flatness, existing WA methods might fall into worse final performances or require extra test-time computations. This work unveils the full potential of EMA with *a single line of modification*, i.e., switching the EMA parameters to the original model after each epoch, dubbed as Switch EMA (SEMA). From both theoretical and empirical aspects, we demonstrate that SEMA can help DNNs to reach generalization optima that better trade-off between flatness and sharpness. To verify the effectiveness of SEMA, we conduct comparison experiments with discriminative, generative, and regression tasks on vision and language datasets, including image classification, self-supervised learning, object detection and segmentation, image generation, video prediction, attribute regression, and language modeling. Comprehensive results with popular optimizers and networks show that SEMA is a free lunch for DNN training by improving performances and boosting convergence speeds.

1. Introduction

Deep neural networks (DNNs) have revolutionized popular application scenarios like computer vision (CV) (He et al., 2017) and natural language processing (NLP) (Devlin et al., 2018) in the past decades. As the size of models and datasets grows simultaneously, it becomes increasingly vital to develop efficient optimization algorithms for better generalization capabilities. A better understanding of the optimization properties and loss surfaces could motivate us to improve the training process and final performances.

^{*}Equal contribution ¹AI Lab, Research Center for Industries of the Future, Westlake University, Hangzhou, China ²DAMO Academy, Alibaba Group, Hangzhou, China ³College of Computer Science and Technology, Zhejiang University, Hangzhou, China. Correspondence to: Stan Z. Li <stan.z.li@westlake.edu.cn>.

Table 1: Comprehensive comparison of optimization and regularization methods from the aspects of pluggable (easy to migrate or not), free gains (performance gain without extra cost or not), speedup (boosting convergence speed or not), and the optimization property (flatness or sharpness).

Type	Method	Pluggable	Free gains	Speedup	Properties
Optimizer	SAM	✓	✗	✗	sharpness
	SASAM	✗	✗	✗	both
	Adan	✗	✗	✓	sharpness
	Lookahead	✓	✓	✓	sharpness
Regularization	SWA	✓	✓	✗	flatness
	EMA	✓	✓	✓	flatness
	SEMA	✓	✓	✓	both

The complexity and high-dimensional parameter space of modern DNNs has posed great challenges in optimization, such as gradient vanishing or exploding, overfitting, and de-generation of large batch size (You et al., 2020). To address these obstacles, two branches of research have been conducted: improving *optimizers* or enhancing optimization by *regularization* techniques. According to their characteristics in Tab. 1, the improved optimizers (Kingma & Ba, 2014; Loshchilov & Hutter, 2019; Ginsburg et al., 2018; Zhang et al., 2019; Foret et al., 2021) tend to be more expensive and focus on sharpness(deeper optimal) by refining the gradient, while the popular regularizations (Srivastava et al., 2014; Cubuk et al., 2019; Zhang et al., 2018; Izmailov et al., 2018; Polyak & Juditsky, 1992) are cheaper to use and focus on flatness(wider optimal) by modifying parameters. More precisely, the optimization strategies from both gradient and parameter perspectives show their respective advantages.

Therefore, a question that deserves to be considered: **is it possible to propose a strategy to optimize both sharpness and flatness simultaneously without incurring additional computational overhead?** Due to simplicity and versatility, the ideal candidate would be weighted averaging (WA) methods (Izmailov et al., 2018; Polyak & Juditsky, 1992) with vanilla optimizers, widely adopted network regularizers that seek local minima at flattened basins by ensemble model weights. However, previous Weight Averaging (WA) techniques either introduced additional computational overhead, as in the case of TWA (Li et al., 2023b), or operated independently of model optimization, like EMA and SWA, thus maintaining unchanged overall efficiency. The limitations of directly using EMA or SWA during training,

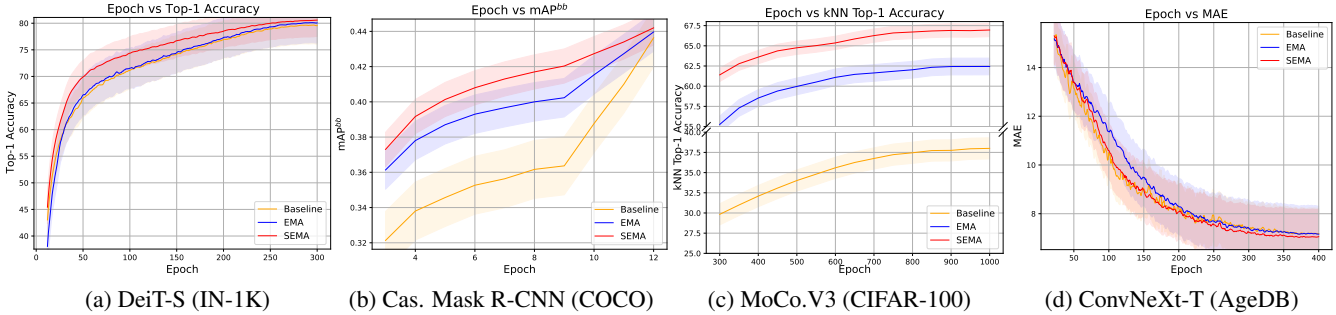


Figure 1: Training epoch vs. performance plots of the **baseline**, **EMA**, and **SEMA**. (a) Image classification with DeiT-S on ImageNet-1K (IN-1K); (b) Object detection and segmentation with ResNet-50 Cascade (Cas.) Mask R-CNN (3×) on COCO; (c) Contrastive learning (CL) pre-training with MoCo.V3 and DeiT-S on CIFAR-100; (d) Face age regression with ResNet-50 on AgeDB. SEMA shows faster convergence speeds and better performances than EMA and the baselines.

which converge quickly but have poor final performance, are underscored by studies like LAWA (Kaddour, 2022) and PSWA (Guo et al., 2022). Techniques like SASAM (Kaddour et al., 2022) indicate that WA can be combined with optimizers to enhance final performance. Consequently, the main objective of this paper is to introduce WA into the optimization process, aiming to expedite convergence while implementing plug-and-play regularization without incurring excessive overhead. In addition to the issue of computational efficiency, we are also inspired by the two-stage optimization strategy of fast and slow: the fast model is used to explore the spiky regions where the empirical risk is minimal (*i.e.*, sharpness), whereas the slow model selects the direction where the risk is more homogeneous (*i.e.*, flatness) for the next update. For example, in regular training utilizing EMA, the fast model corresponds to a model that rapidly updates towards the target in each local iteration, while the slow model precisely aligns with the EMA model. They all have ideal optimization properties but lack the enhancement of interaction during training.

Hence, we introduce *Switch Exponential Moving Average* (SEMA) as a dynamic regularizer, which incorporates flatness and sharpness by switching fast and slow models at the end of each training epoch. At each training stage of switching, SEMA fully utilizes the fast convergence of EMA to reach flat local minima, as shown in Figure 1, allowing the optimizer to further explore lower basins through sharp trajectories based on previous EMA parameters for better generalization. In extensive experiments with different tasks and various network architectures, including image classification, self-supervised learning, object detection and segmentation, image generation, regression, video prediction, and language modeling, SEMA improves the performance of baselines consistently as a plug-and-play free lunch. In summary, we make the following contributions:

- We propose the Switch Exponential Moving Average (SEMA) method, and through visualization of the loss landscape and decision boundary experiments, we demonstrate its effectiveness in improving model perfor-

mance across various scenarios.

- We first apply weight averaging to the training dynamics, allowing SEMA to take both flatness and sharpness into account simultaneously, facilitating faster convergence.
- Comprehensive empirical evidence proves the effectiveness of SEMA. Across various tasks and datasets, SEMA surpasses state-of-the-art baseline models and outperforms alternative optimization methods.

2. Related Work

Optimizers. With backward propagation (BP) (Rumelhart et al., 1986) and stochastic gradient descending (SGD) (Sinha & Griscik, 1971) with mini-batch training (Bishop, 2006), optimizers play a crucial part in the training process of DNNs. Mainstream optimizers utilize momentum techniques (Sutskever et al., 2013) for gradient statistics and improve DNNs’ convergence and performance by adaptive learning rates (*e.g.*, Adam variants (Kingma & Ba, 2014; Liu et al., 2020)) and acceleration schemes (Kobayashi, 2020). SAM (Foret et al., 2021) aims to search a flatter region where training losses in the estimated neighborhood by solving min-max optimizations, and its variants improve training efficiency (Liu et al., 2022a) from aspects of gradient decomposition (Zhuang et al., 2022), training costs (Du et al., 2021; 2022). To accelerate training, large-batch optimizers like LARS (Ginsburg et al., 2018) for SGD and LAMB (You et al., 2020) for AdamW (Loshchilov & Hutter, 2019) adaptively adjust the learning rate based on the gradient norm to achieve faster training. Adan (Xie et al., 2023) introduces Nesterov descending to AdamW, bringing improvements across popular CV and NLP applications. Another line of research proposes plug-and-play optimizers, *e.g.*, Lookahead (Zhang et al., 2019; Zhou et al., 2021) and Ranger (Wright, 2019), combining with existing inner-loop optimizers (Zhou et al., 2021) and working as the outer-loop optimization.

Weight Averaging. In contrast to momentum updates of gradients in optimizers, weight averaging (WA) techniques,

e.g., SWA (Izmailov et al., 2018) and EMA (Polyak & Juditsky, 1992), are commonly used in DNN training to improve model performance. As test-time WA strategies, SWA variants (Maddox et al., 2019) and FGE variants (Guo et al., 2023; Garipov et al., 2018) heuristically ensemble different models from multiple iterations (Granzio et al., 2021) to reach flat local minima and improve generalization capacities. TWA (Li et al., 2023b) improves SWA by a trainable ensemble. Model soup (Wortsman et al., 2022) is another WA technique designed for large-scale models, which greedily ensembles different fine-tuned models and achieves significant improvements. When applied during training, EMA update (*i.e.*, momentum techniques) can improve the performance and stabilities. Popular semi-supervised learning (e.g., FixMatch variants (Sohn et al., 2020)) or self-supervised learning (SSL) methods (e.g., MoCo variants (He et al., 2020; Chen et al., 2021), and BYOL variants (Grill et al., 2020)) utilize the self-teaching framework, where the parameters of teacher models are the EMA version of student models. In reinforcement learning, A3C (Mnih et al., 2016) applies EMA to update policy parameters to stabilize the training process. EMA significantly contributes to the stability and output distribution in generative models like diffusion (Karras et al., 2023). Moreover, LAWA (Kaddour, 2022) and PSWA (Guo et al., 2022) try to apply EMA or SWA directly during the training process and found that using WA during training only accelerates convergence rather than guarantee final performance gains. SASAM (Kaddour et al., 2022) combines the complementary merits of SWA and SAM for better local flatness. Nevertheless, since these WA techniques are universal and easy to migrate, they remain crucial for innovation. We improve EMA by leveraging the historical exploration of a single configuration, prioritizing training efficiency to achieve faster convergence.

Regularizations. Network parameter regularizations, *e.g.*, weight decay (Andriushchenko et al., 2023), dropout variants (Srivastava et al., 2014; Huang et al., 2016), and normalization techniques (Peng et al., 2018; Wu & Johnson, 2021), control model complexity and stabilities to prevent overfitting and are proven effective in improving model generalization. The WA algorithms also fall into this category. For example, EMA can effectively regularize Transformer (Devlin et al., 2018; Touvron et al., 2021) training in both CV and NLP scenarios (Liu et al., 2022d; Wightman et al., 2021). Another part of important regularization techniques aims to improve generalizations by modifying the data distributions, such as label regularizers (Szegedy et al., 2016)) and data augmentations (DeVries & Taylor, 2017). Both data-dependant augmentations like Mixup variants (Zhang et al., 2018; Yun et al., 2019; Liu et al., 2022c) and data-independent methods like RandAugment variants (Cubuk et al., 2019; 2020)) enlarge data capacities and diversities, yielding significant performance gains while introducing ignorable additional computational overhead. Most regu-

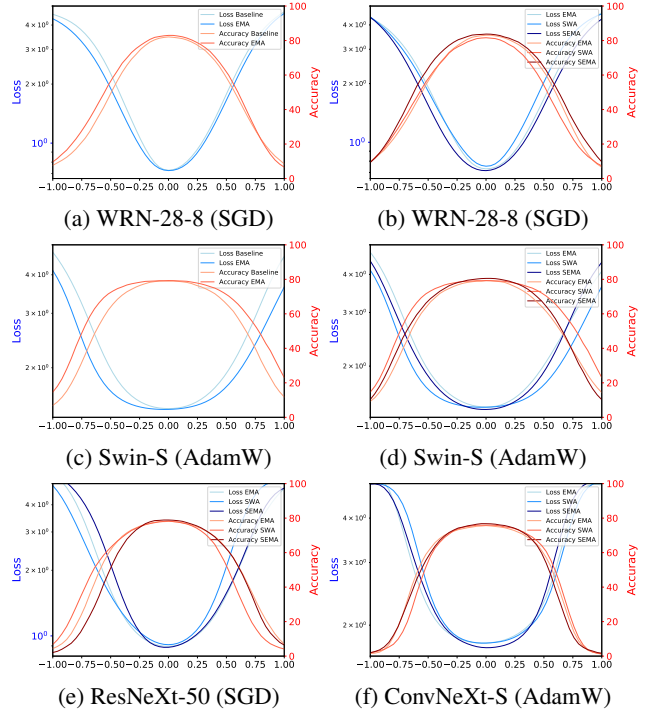


Figure 2: 1D loss landscape with validation **loss** and top-1 **accuracy** of classification on CIFAR-100. The loss landscapes of EMA and SWA models are flatter than those of the baseline (using vanilla optimizers), while the proposed SEMA yields deeper and smoother landscapes.

larization methods provide “free lunch” solutions that effectively improve performance as a pluggable module with no extra costs. Our proposed SEMA is a new “free-lunch” regularization method that improves generalization abilities as a plug-and-play step for various application scenarios.

3. Switch Exponential Moving Average

We present the Switch Exponential Moving Average (SEMA) and analyze its properties. In section 3.1, we consider both the performance and landscape of optimizers (*e.g.*, SGD and AdamW) with or without EMA, which helps understand the loss geometry of DNN training and motivates the SEMA procedure. Then, in section 3.2, we formally introduce the SEMA algorithm. We also derive its practical consequences after applying SEMA to conventional DNN training. Finally, in section 3.3, we provide the theoretical analysis for proving the effectiveness of SEMA.

3.1. Loss Landscape Analysis

SEMA is based on the dynamic weight averaging of switching the slow model generated by EMA to the fast model optimized directly by the optimizer in a specific interval that allows the combination of each unique characteristic to form an intrinsically efficient learning scheme. Therefore, with the popular CNNs and ViTs as backbones, we first analyze

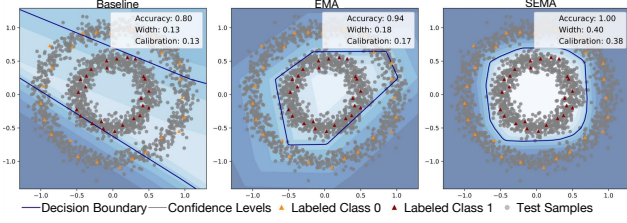


Figure 3: Illustration of the baseline, EMA, and SEMA on Circles Dataset with 50 labeled samples (triangle red/yellow points) with others as testing samples (gray points) in training a 2-layer MLP. We plot the decision boundary, accuracy, decision boundary width, and prediction calibration.

the loss landscape and performance to motivate our method.

EMA. As a special case of moving average, applies weighting factors that decrease exponentially. Formally, with a momentum coefficient $\alpha \in (0, 1)$ as the decay rate, an EMA recursively calculates the output model weight:

$$\theta_t^{\text{EMA}} = \alpha \cdot \theta_t^{\text{Opt}} + (1 - \alpha) \cdot \theta_{t-1}^{\text{EMA}} \quad (1)$$

where θ is the model parameters, and t is the iteration step in training. A higher α discounts older observations faster.

Loss Landscape. The method of visualizing the loss landscape is based on linear interpolation of models (Li et al., 2018) to study the “sharpness” and “flatness” of different minima. Assuming there is a center point θ^* as the local minima of the loss landscape and one direction vector η , the formulation of plotting the loss function \mathcal{L} is:

$$f(\alpha) = \mathcal{L}(\theta^* + \alpha \cdot \eta) \quad (2)$$

For each learned model, the 1-dimensional landscape can be defined by the weight space of the final model. As shown in Figure 2, models are trained by optimizers (SGD or AdamW) with or without EMA on CIFAR-100. There are two interesting observations: **(a) the vanilla optimizer without EMA produces a higher and steeper peak, whereas (b) with EMA, it has a smoother curve with a lower peak.** These two methods perfectly connect to the two basic properties of loss landscape, flatness and sharpness, which could be the key to reaching the desired solution of deeper and wider optima for better generalization. The proposed SEMA combines the two advantages without extra computation cost. We further demonstrate the beneficial consequences of using SEMA in the next subsection.

3.2. Switch EMA Algorithm

We now present the proposed Switch Exponential Moving Average algorithm, a simple but effective modification for training DNNs. Based on conclusions in section 3.1, since EMA is independent of the learning objective and will stack in the basin without local sharpness, *i.e.*, failing to explore local minima further. Intuitively, the key issue lies in how to

make the slow EMA model θ^{EMA} optimizable along with the fast model θ^{Opt} during the training process. Therefore, we introduce the simple switching operation between the two models to achieve this goal, *i.e.*, switching θ^{Opt} to θ^{EMA} regularly according to a predefined switching interval T . Formally, SEMA can be summarized as follows:

$$\begin{aligned} \theta'_t &= \theta_{t-1}^{\text{SEMA}} - \eta \nabla \mathcal{L}(\theta_{t-1}^{\text{SEMA}}), \\ \theta_t^{\text{SEMA}} &= \begin{cases} \theta'_t, & t \% T = 0 \\ \alpha \cdot \theta'_t + (1 - \alpha) \cdot \theta_{t-1}^{\text{SEMA}}, & t \% T \neq 0 \end{cases} \end{aligned}$$

where θ' is an intermediate optimizer iterate. Practically, we set T to the multiple of the iteration number for traversing the whole dataset, *e.g.*, switching by each epoch. The training procedure of SEMA is summarized in Algorithm 1, where we only add a line of code to the EMA algorithm.

Three practical consequences of such simple modification on the vanilla optimization process are summarized as follows:

Faster Convergence. SEMA significantly boosts the convergence speed of DNN training. As demonstrated by the 2D loss landscapes in Figure 4, the baseline model frequently gets stuck on the edge of a cliff. In contrast, the EMA model quickly reaches a flat basin. However, when plotted on the SEMA landscape, the model approaches the local minimum via a steeper path, while the EMA model swiftly arrives at a flat, albeit inferior, region. This suggests that SEMA can guide the optimization process towards better solutions, achieving lower losses and reaching the local basin with more efficient strategies and fewer training steps.

Better Performance. SEMA enhances the performance of DNNs by skillfully leveraging the strengths of both the baseline and EMA models. SEMA exhibits a deeper and more distinct loss landscape compared to the baseline and existing WA methods, as illustrated in Figure 2b. This starkly contrasts with the EMA, which only shows flatness, and SWA models trained with the straightforward optimizer. This unique characteristic allows SEMA to explore solutions with superior local minima, thereby improving its generalization across a range of tasks. Intriguingly, SEMA maintains this sharper landscape under different optimizers/backbones 2c. In fact, the loss landscapes 2d of EMA and SWA models appear flatter than that of the baseline.

Smoother Decision. SEMA can produce smoother decision boundaries, enhancing the robustness of the trained models. Figure 3 visualizes the decision boundaries on a toy dataset and illustrates that SEMA models demonstrate greater regularity compared to EMA models. Conversely, EMA models may have more jagged decision boundaries. The smoother decision boundaries produced by SEMA allow for more reliable and consistent predictions, even in regions with complex data distributions. As confirmed by Figure 2b, the smoother decision boundaries generated by

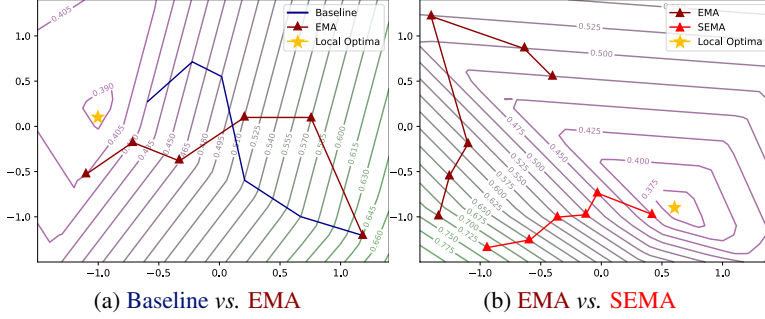


Figure 4: Illustration of 2D loss landscape and optimization trajectory on Circles test set. EMA models reach the flat basin while the baseline is stuck at the sharp cliff. Projecting the EMA model to the landscape of SEMA, the SEMA model approaches the local minima efficiently.

SEMA can enhance the model’s performance. This is particularly evident in tasks requiring fine-grained classification or complex data distributions. Smooth boundaries reduce the chance of overfitting to noise and data variations. This, in turn, ensures more reliable and consistent predictions, further solidifying SEMA’s advantage over other models.

3.3. Theoretical Analysis

To further substantiate the behavior and advantages of SEMA compared to existing optimization and WA methods in stochastic optimization scenarios and to verify its training stability and convergence characteristics, we take SGD as an example and present a theoretical analysis from two aspects. Let η be the learning rate of the optimizer α be the decay rate of SGD, EMA, and SEMA. In the noise quadratic model, the loss of iterates Θ_t is defined as:

$$\mathcal{L}(\Theta_t) = \frac{1}{2}(\Theta_t - c)^T A(\Theta_t - c), \quad (3)$$

where $c \sim \mathcal{N}(\theta^*, \Sigma)$ and A is the coefficient matrix of the \mathcal{L} with respect to Θ . Without loss of generality, we set $\theta^* = 0$. We denote the models learned by SGD, EMA, and SEMA as θ_t^{SGD} , θ_t^{EMA} , and θ_t^{SEMA} , respectively.

Proposition 1. (Low-frequency Oscillation): In the noisy quadratic model, the variance of SGD, EMA, and SEMA iterates, denoted as V_{SGD} , V_{EMA} and V_{SEMA} , converge to the following values according to Banach’s fixed point theorem, and, $V_{SEMA} < V_{EMA} < V_{SGD}$:

$$\begin{aligned} V^{SGD} &= \frac{\eta A}{2I - \eta A} \Sigma, \\ V^{EMA} &= j \cdot V^{SGD}, \\ V^{SEMA} &= k \cdot V^{EMA}. \end{aligned} \quad (4)$$

where $j < 1$ and $k < 1$ are the coefficients, $j = \frac{\alpha}{2-\alpha} \cdot \frac{2-\alpha-(1-\alpha)\eta A}{\alpha+(1-\alpha)\eta A}$, and $k = \frac{2-\alpha}{\alpha} \cdot \frac{\alpha+(1-\alpha)\eta A}{2-\alpha-(1-\alpha)\eta A} \cdot \frac{\alpha\eta A}{2I-\eta A}$. Practically, SEMA’s stability can be traced back to its ability to mitigate low-frequency oscillations during

Algorithm 1 Pytorch-style pseudocode for SEMA.

```
# f, f_ema: original and EMA networks
# m: EMA momentum coefficient
f.params = f_ema.params # initialization
for i in N epochs: # N epochs in total
    for x, y in loader: # load a minibatch
        loss = LossFunction(f(x), y)
        # optimization and update f.params
        loss.backward()
        optimizer.step()
        # momentum update f_ema.params
        f_ema.params = (1-m)*f.params + m*f_ema.params
    Evaluate(f_ema) # evaluation on validation set
    # update f.params as f_ema.params
    f.params = f_ema.params
```

optimization. The proposition demonstrates that SEMA achieves a lower variance compared to EMA and SGD. A lower variance signifies a more stable optimization trajectory, indicating smoother parameter updates and less erratic behavior. As illustrated in Figure 4, SEMA facilitates steady progress towards a local minimum without being impeded by slow and irregular parameter updates. The proof of Proposition 1 is provided in Appendix A.1.

Proposition 2. (Fast Convergence): The iterative update of SEMA ensures its gradient descent property as SGD, which EMA doesn’t have. It can be formulated as:

$$(\theta_{t+1}^{SEMA} - \theta_t^{SEMA}) \propto -\nabla \mathcal{L}(\theta_t^{SGD}) \quad (5)$$

Practically, the stability and accelerated convergence of SEMA can be attributed to its ability to integrate the fundamental gradient descent characteristic with rapid convergence. As demonstrated by the proposed proposition and Figure 4, SEMA’s iterative update is proportional to the negative gradient of the loss function. This signifies that SEMA blends the baseline gradient descent characteristic with accelerated convergence, thereby ensuring that the optimization process evolves toward loss reduction and achieves faster convergence. In contrast, EMA does not share the same gradient descent characteristics as SGD. EMA incorporates a smoothing factor that blends current parameter estimates with previous estimates, resulting in a more gradual convergence. Proposition 2 is proofed by Appdenix A.2.

4. Experiments

4.1. Experimental Setup

We conduct extensive experiments across a wide range of popular application scenarios to verify the effectiveness of SEMA. Taking vanilla optimizers as the baseline (basic), the compared regularization methods plugged upon the baseline include EMA (Polyak & Juditsky, 1992), SWA (Izmailov et al., 2018), and Lookahead optimizers (Zhang et al., 2019). We use the momentum coefficients of 0.9999 and 0.999 for EMA and SEMA, 1.25 budge for SWA, and one epoch

Table 2: Classification with top-1 accuracy (Acc, %)↑ and performance gains on ImageNet-1K based on various backbones, optimizers, and training epochs (ep). R, CX, and Moga denote ResNet, ConvNeXt, and MogaNet.

Backbone	R-50	R-50	R-50	R-50	DeiT-T	DeiT-S	Swin-T	CX-T	Moga-B	DeiT-S	DeiT-B	DeiT-S	DeiT-B	CX-T
Optimizer	SGD	SAM	LARS	LAMB	AdamW	AdamW	AdamW	AdamW	AdamW	LAMB	LAMB	Adan	Adan	Adan
	100ep	100ep	100ep	300ep	300ep	300ep	300ep	300ep	300ep	100ep	100ep	150ep	150ep	150ep
Basic	76.8	77.2	78.4	79.8	73.0	80.0	81.2	82.1	84.5	74.1	76.1	79.3	81.0	81.3
+EMA	77.0	77.3	78.4	79.7	73.0	80.2	81.3	82.1	84.6	73.9	77.3	79.4	81.1	81.6
+SEMA	77.1	77.4	78.6	79.9	73.2	80.6	81.6	82.2	84.8	74.4	77.4	79.5	81.3	81.7
Gains	0.3	0.2	0.2	0.1	0.2	0.6	0.4	0.1	0.3	0.3	1.3	0.2	0.3	0.4

switch interval for SEMA. As for the vanilla optimizers, we consider SGD variants (momentum SGD (Sinha & Griscik, 1971) and LARS (Ginsburg et al., 2018)) and Adam variants (Adam (Kingma & Ba, 2014), AdamW (Loshchilov & Hutter, 2019), LAMB (You et al., 2020), SAM (Foret et al., 2021), Adan (Xie et al., 2023)). View Appendix B for details of implementations and hyperparameters. All experiments are implemented with PyTorch and run on NVIDIA A100 or V100 GPUs, and we use the **bold** and **grey** backgrounds as the best result and the default baselines. The reported results are averaged over three trials. We intend to verify three empirical merits of SEMA: (i) **Convenient plug-and-play usability.**, as the basic optimization methods we compared, SEMA enables convenient plug-and-play; (ii) **Higher performance gains.**, SEMA can take into account both flatness and sharpness, which makes it more able to converge the local optimal position than other optimization methods, thus bringing higher performance gains to the model; (iii) **Faster convergence.**, SEMA also has gradient descent, which allows it to help models converge faster.

Table 3: Classification with top-1 accuracy (%)↑ and performance gains on CIFAR-100 based on various backbones.

Backbone	Basic	+EMA	+SWA	+Lookahead	+SEMA	Gains
R-18	76.91	77.16	77.13	77.07	77.61	0.70
RX-50	79.06	79.21	79.25	79.28	79.80	0.74
R-101	76.90	77.48	77.41	77.27	77.62	0.72
WRN-28-10	81.94	82.27	81.16	81.20	82.35	0.41
DenseNet-121	80.49	80.70	80.83	80.74	81.05	0.56
DeiT-S	63.34	64.46	64.17	64.25	64.58	1.24
MLPMixer-T	78.22	78.49	78.54	78.33	78.84	0.62
Swin-T	79.07	79.17	79.30	79.28	79.74	0.67
Swin-S	78.25	79.08	78.93	78.76	79.30	1.05
ConvNeXt-T	78.37	79.24	78.96	78.82	79.42	1.05
ConvNeXt-S	60.18	61.45	61.04	60.29	61.76	1.58
MogaNet-S	83.69	83.92	83.78	83.67	84.02	0.33

4.2. Experiments for Computer Vision Tasks

We first apply WA regularizations to comprehensive vision scenarios that cover discriminative, generation, predictive, and regression tasks to demonstrate the versatility of SEMA on CIFAR-10/100 (Krizhevsky et al., 2009), ImageNet-1K (IN-1K) (Deng et al., 2009), STL-10 (Coates et al., 2011), COCO (Lin et al., 2014), CelebA (Liu et al., 2015), IMDB-WIKI (Rothe et al., 2018), AgeDB (Moschoglou et al., 2017), RCFMNIST (Yao et al., 2022), and Moving MNIST (MMNIST) (Srivastava et al., 2015) datasets.

Image classification. Evaluations are carried out from two perspectives. Firstly, we verify popular network architectures on the standard CIFAR-100 benchmark with 200-epoch training: (a) classical Convolution Neural Networks (CNNs) include ResNet-18/101 (R) (He et al., 2016), ResNeXt-50-32x4d (RX) (Xie et al., 2017), Wide-ResNet-28-10 (WRN) (Zagoruyko & Komodakis, 2016), and DenseNet-121 (Huang et al., 2017); (b) Transformer (Metaformer) architectures includes DeiT-S (Touvron et al., 2021), Swin-T/S (Liu et al., 2021), and MLP-Mixer-T (Tolstikhin et al., 2021); (c) Modern CNNs include ConvNeXt-T/S (CX) (Liu et al., 2022d) and MogaNet-S (Moga) (Li et al., 2024b). Note that classical CNNs are trained by SGD optimizer with 32^2 resolutions, while other networks are optimized by AdamW with 224^2 input size. Table 3 notably shows that SEMA consistently achieves the best top-1 Acc compared to WA methods and Lookahead across 12 backbones, where SEMA also yields fast convergence speeds in Figure 1. Then, we further conduct large-scale experiments on IN-1K to verify various optimizers (e.g., SGD, SAM, LARS, LAMB, AdamW, and Adan) using standardized training procedures and the networks mentioned above. In Table 2, SEMA enhances a wide range of optimizers and backbones, e.g., +0.6/1.3/0.4% Acc upon DeiT-S/DeiT-B/CX-T with AdamW/LAMB/Adan, while conducting Acc gains in situations where EMA is not applicable (e.g., R-50 and DeiT-S with LAMB). View Appendix B.1 for details.

Table 4: Pre-training with top-1 accuracy (%)↑ of linear probing (Lin.) or fine-tuning (FT) and performance gains on CIFAR-100 and STL-10 based on various SSL algorithms.

Self-sup	Dataset	Backbone	Basic	+EMA	+SWA	+SEMA	Gains
SimCLR	CIFAR-100	R-18	67.18	58.46	57.82	67.28	0.10
SimCLR	STL-10	R-50	91.77	82.82	91.36	92.93	1.16
MoCo.V2	CIFAR-100	R-18	62.34	66.53	62.85	66.56	0.03
MoCo.V2	STL-10	R-50	91.33	91.36	91.40	91.48	0.12
BYOL	CIFAR-100	R-18	55.09	69.60	56.36	69.86	0.26
BYOL	STL-10	R-50	75.76	93.24	76.29	93.48	0.24
BarlowTwins	CIFAR-100	R-18	65.49	60.13	60.53	65.55	0.06
BarlowTwins	STL-10	R-50	88.67	80.11	88.35	88.80	0.13
MoCo.V3	CIFAR-100	DeiT-S	38.09	46.79	39.61	52.27	5.48
MoCo.V3	STL-10	DeiT-S	61.88	79.25	62.49	80.44	1.19
SimMIM	CIFAR-100	DeiT-S	81.96	82.05	81.77	82.15	0.19
SimMIM	STL-10	DeiT-S	91.88	69.14	78.23	92.06	0.18
A ² MIM	CIFAR-100	DeiT-S	82.28	82.14	82.05	82.46	0.18
A ² MIM	STL-10	DeiT-S	92.27	70.88	80.64	93.33	1.06

Self-supervised Learning. Since EMA plays a vital role in some SSL methods, we also evaluate WA methods with

Table 5: Pre-training (PT) with top-1 accuracy (%) \uparrow of linear probing or FT and performance gains on IN-1K based on various SSL methods with various PT epochs.

Dataset	Backbone	PT	Basic	+EMA	+SWA	+SEMA	Gains
BYOL	R-50	200ep	65.49	69.78	66.37	69.96	0.18
MoCo.V3	DeiT-S	300ep	67.73	71.77	68.54	72.01	0.24
SimMIM	DeiT-B	800ep	83.85	83.94	83.79	84.16	0.31
MAE	DeiT-B	800ep	83.33	83.37	83.35	83.48	0.15

two categories of popular SSL methods on CIFAR-100, STL-10, and IN-1K, *i.e.*, contrastive learning (CL) methods include SimCLR (Chen et al., 2020a), MoCo.V2 (Chen et al., 2020b), BYOL (Grill et al., 2020), Barlow Twins (BT) (Zbontar et al., 2021), and MoCo.V3 (Chen et al., 2021), which are tested by linear probing (Lin.), and masked image modeling (MIM) include MAE (He et al., 2022), SimMIM (Xie et al., 2022), and A²MIM using fine-tuning (FT) protocol. Notice that most CL methods utilize ResNet variants (optimized by SGD or LARS) as the encoders, while MoCo.V3 and MIM algorithms use ViT backbones (optimized by AdamW). Firstly, we perform 1000-epoch training on small-scale datasets with 224² resolutions for fair comparison in Table 4, where SEMA performs best upon CL and MIM methods. When EMA is used in self-teaching frameworks (MoCo.V2/V3 and BYOL), SEMA improves EMA by 0.12~5.48% Acc on STL-10 where SWA fails to. When EMA and SWA showed little gains or negative effects upon MIM methods, SEMA still improves them by 0.18~1.06%. Then, we compare WA methods on IN-1K with larger encoders (ResNet-50 and ViT-S/B) using the standard pre-training settings. As shown in Table 5, SEMA consistently yields the most performance gains upon CL and MIM methods. View Appendix B.2 for details.

Table 6: Object detection and instance segmentation with mAP^{bb} (%) \uparrow , mAP^{mk} (%) \uparrow , and performance gains on COCO based on Mask R-CNN variants using ResNet-50.

Method	Basic		+EMA		+SEMA		Gains	
	AP ^{bb}	AP ^{mk}	AP ^{bb}	AP ^{mk}	AP ^{bb}	AP ^{mk}	AP ^{bb}	AP ^{mk}
Mask R-CNN (2 \times)	39.1	35.3	39.3	35.5	39.7	35.8	0.6	0.5
Cas. Mask R-CNN (3 \times)	44.0	38.3	44.2	38.5	44.4	38.6	0.4	0.3
Cas. Mask R-CNN (9 \times)	44.0	38.5	44.5	38.8	45.1	39.2	1.1	0.7

Table 7: Object detection with mAP^{bb} (%) \uparrow and performance gains on COCO based on various detection methods.

Method	Backbone	Basic	+EMA	+SWA	+SEMA	Gains
RetinaNet (2 \times)	R-50	37.3	37.6	37.6	37.7	0.4
RetinaNet (1 \times)	Swin-T	41.6	41.8	41.9	42.1	0.5
YoloX (300ep)	YoloX-S	37.7	40.2	39.6	40.5	0.3

Object Detection and Instance Segmentation. As WA methods (Zhang et al., 2020) were verified useful in detection (Det) and segmentation (Seg) tasks, we benchmark them on COCO with two types of training settings. Firstly, using the standard fine-tuning protocol in MMDetection (Chen et al., 2019), RetinaNet (Lin et al., 2017), Mask R-CNN (He et al., 2017), and Cascade Mask R-CNN

(Cas.) (Cai & Vasconcelos, 2019) are fine-tuned by SGD or AdamW with IN-1K pre-trained R-50 or Swin-T encoders, as shown in Table 6 and Table 7. SEMA achieved substantial gains of AP^{bb} and AP^{mk} over the baseline model in all methods and exceeded gains of EMA models. Then, we train YoloX-S detector (Ge et al., 2021) from scratch by SGD optimizer for 300 epochs in Table 7. It takes EMA as part of its training strategy, where EMA significantly improves the baseline by 2.5% AP^{bb}, while SEMA further improves EMA by 0.3% AP^{bb}. View Appendix B.3 for details.

Table 8: Image generation with FID (%) \downarrow and performance gains on CIFAR-10 and CelebA-Align based on DDPM.

Dataset	Basic	+EMA	+SWA	+Lookahead	+SEMA	Gains
CIFAR-10	7.17	5.43	6.35	6.84	5.30	0.13
CelebA-Align	7.90	7.49	7.53	7.67	7.11	0.38

Table 9: Video prediction with MSE \downarrow , PSNR \uparrow , and performance gains on MMNIST based on various methods.

Method	Basic		+EMA		+SEMA		Gains (%)	
	MSE	PSNR	MSE	PSNR	MSE	PSNR	MSE	PSNR
SimVP	32.15	21.84	32.14	21.84	32.06	21.85	0.28	0.05
SimVP.V2	26.70	22.78	27.12	22.75	26.68	22.81	0.07	0.13
ConvLSTM	23.97	23.28	24.06	23.27	23.92	23.31	0.21	0.13
PredRNN	29.80	22.10	29.76	22.15	29.73	22.16	0.23	0.27

Table 10: Regression tasks with MAE \downarrow , RMSE \downarrow , and performance gains on RCF-MNIST, AgeDB, and IMDB-WIKI based on various backbone (back.) encoders.

Dataset	Back.	Basic		+EMA		+SWA		+SEMA		Gains (%)	
		MAE	RMSE	MAE	RMSE	MAE	RMSE	MAE	RMSE	MAE	RMSE
RCF-MNIST R-18		5.61	27.30	5.50	27.70	5.53	27.73	5.41	26.79	3.57	1.79
RCF-MNIST R-50		6.20	28.78	5.81	27.19	6.04	27.87	5.74	27.71	7.42	3.72
AgeDB R-50		7.25	9.50	7.33	9.62	7.37	9.59	7.22	9.49	0.41	0.11
AgeDB CX-T		7.14	9.19	7.31	9.39	7.28	9.34	7.13	9.13	0.14	0.65
IMDB-WIKI R-50		7.46	11.31	7.50	11.24	7.62	11.45	7.49	11.11	0.40	1.77
IMDB-WIKI CX-T		7.72	11.67	7.21	10.99	7.87	11.71	7.19	10.94	6.86	6.26

Image Generation. Then, we evaluate image generation (Gen) tasks based on DDPM (Ho et al., 2020) on CIFAR-10 and CelebA-Align because EMA significantly enhances diffusion models. Table 8 shows that FID drops dramatically without using EMA. SEMA can yield considerable FID gains and outperform other optimization methods on all datasets. View Appendix B.4 for details.

Video Prediction. Based on OpenSTL benchmark (Tan et al., 2023), we verify the video prediction (VP) task on MMNIST based on various VP methods. Table 9 shows that SEMA can improve MSE and PSNR metrics for recurrent-based (ConvLSTM (Shi et al., 2015) and PredRNN (Wang et al., 2017)) and recurrent-free models (SimVP and SimVP.V2 (Gao et al., 2022)) compared to the baseline while other WA methods usually cost performance degradation. View Appendix B.5 for details.

Visual Attribute Regression. We further evaluate face age regression tasks on AgeDB (Moschoglou et al., 2017) and IMDB-WIKI (Rothe et al., 2018) and pose regression

Table 11: Language processing with perplexity↓ on Penn Treebank based on 2-layer LSTM.

Optimizer	Basic	+EMA	+SWA	+SEMA	Gains
SGD	67.5	67.3	67.4	67.1	0.4
Adam	67.3	67.2	67.1	67.0	0.3
AdaBelief	66.2	66.1	66.0	65.9	0.3

Table 12: Text classification and languaging modeling with Acc (%)↑ and perplexity↓ on Yelp Review and WikiText-103 based on BERT-Base.

Dataset	Metric	Basic	+EMA	+SWA	+SEMA	Gains
Yelp Review	Acc↑	68.26	68.35	68.38	68.46	0.20
WikiText-103	Perplexity↓	29.92	29.57	29.60	29.46	0.46

on RCFMNIST (Yao et al., 2022) using ℓ_1 loss. As shown in Table 10, SEMA achieves significant gains in terms of MAE and RMSE metrics compared to the baseline methods on various datasets, particularly with a 7.42% and 3.72% improvement on the R-50 model trained on the RCF-MNIST dataset and a 6.86% and 6.26% improvement on the CX-T model trained on IMDB-WIKI. Moreover, the experimental results consistently outperform the models trained using EMA and SWA training strategies, details in Appendix B.6.

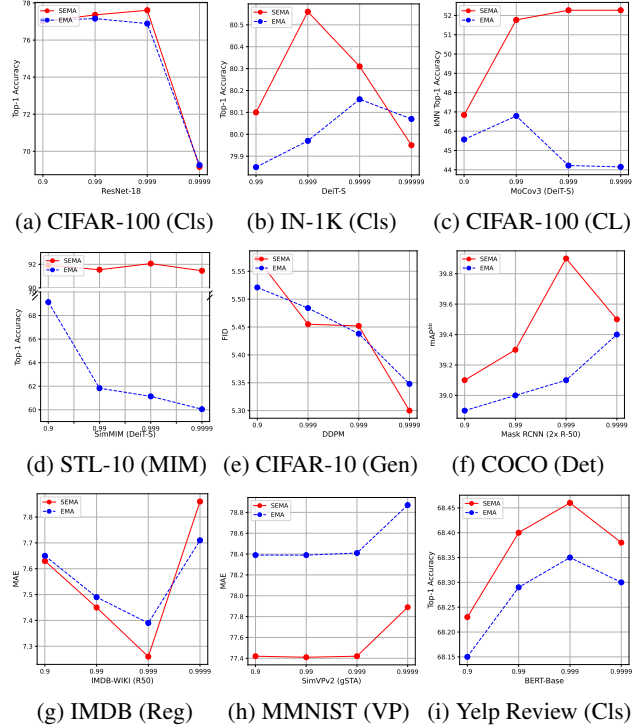
4.3. Experiments for Language Processing Tasks

Then, we also conduct experiments with classical NLP tasks on Penn Treebank, Yelp Review, and WikiText-103 datasets to verify whether the merits summarized above still hold. Following AdaBelief (Zhuang et al., 2020), we first evaluate language processing with 2-layer LSTM (Ma et al., 2015) on Penn Treebank (Marcus et al., 1993) trained by various optimizers in Table 11, indicating the consistent improvements by SEMA. Then, we evaluate fine-tuning with pre-trained BERT-Base (Devlin et al., 2018) backbone for text classification on Yelp Review (Yel) using USB settings (Wang et al., 2022) and language modeling with randomly initialized BERT-Base on WikiText-103 (Ott et al., 2019) uses FlowFormer settings. Table 12 shows that applying SEMA to pre-training or fine-tuning is more efficient than other WA methods. View Appendix B.7 for detailed settings.

4.4. Ablation study

This section analyzes the two hyperparameters α and T in SEMA to verify whether their default values are robust and general enough based on experimental settings in Sec. 4.1.

Momentum Coefficient α . To investigate the effectiveness and generalization of SEMA, we conducted ablation studies with different momentum coefficients on SEMA and EMA, varying from 0.9 to 0.99999 (choosing four continuing values). As shown in Figure 5, SEMA prefers 0.999 in most cases, except for image generation (0.9999) and video prediction (0.9). The preference of α for both EMA and SEMA are robust, and empirical values in different tasks

Figure 5: Ablation of the momentum α in EMA and SEMA, choosing 0.9~0.9999 or 0.99~0.99999.

are provided in Table A1 and Table A2.

Table 13: Ablation of switching interval T (0.5~5 epochs).

T	CIFAR-100		STL-10	IN-1K	CIFAR-10	AgeDB	Yelp
Task	Cls (Acc) \uparrow	CL (Acc) \uparrow	MIM (Acc) \uparrow	Cls (Acc) \uparrow	Gen (FID) \downarrow	Reg (MAE) \downarrow	Cls (Acc) \uparrow
	WRN-28-10	MoCo-V3	SimMIM	DeiT-S	DDPM	R-50	BERT
0.5	82.23	50.73	92.01	79.5	6.07	7.34	68.17
1	82.35	52.27	92.06	80.6	5.30	7.22	68.46
2	82.34	52.25	91.93	80.1	5.33	7.24	68.28
5	82.08	51.94	91.68	78.9	5.28	7.26	68.23

Switching Interval T . We verify whether the one-epoch switching interval is optimal and robust for general usage. Table A3 shows that one epoch switching interval yields the optimal performance in most cases. However, choosing a smaller interval hinders accurate gradient estimation and might disrupt the continuity of optimizer statistics in the Adam series and degenerate performance. On the contrary, larger intervals lead to slower update rates and increased training time, except for specific tasks like diffusion generation that extremely prefer smoothness (Karras et al., 2023).

5. Conclusion

This paper presents SEMA, a highly effective regularizer for DNN optimization that harmoniously blends the benefits of flatness and sharpness. SEMA has shown superior performance gains and versatility across various tasks, including discriminative and generative foundational tasks, regression, and forecasting, and across two modalities. As a pluggable and general method, SEMA expedites convergence and en-

hances final performances without incurring extra computational costs. SEMA marks a significant milestone in DNN optimization, providing a universally applicable solution for a multitude of training tasks in deep learning.

Acknowledgement

This work was supported by National Key R&D Program of China (No. 2022ZD0115100), National Natural Science Foundation of China Project (No. U21A20427), and Project (No. WU2022A009) from the Center of Synthetic Biology and Integrated Bioengineering of Westlake University. This work was done by Juanxi Tian, Zedong Wang, and Weiyang Jin during their internship at Westlake University.

Impact Statements

This paper proposes SEMA, a powerful optimization and regularization technique in deep learning (DL). SEMA offers a pluggable general solution that accelerates convergence and improves model performance without incurring additional computational costs. SEMA marks a significant milestone in DNN optimization, providing a universally applicable solution for a multitude of training tasks in DL. Its practical value lies in its ability to enhance the performance of DNNs across various domains and tasks, making it a valuable tool for researchers and practitioners in designing more effective optimizers and regularization techniques. SEMA’s impact on the deep learning community is inspiring, surpassing state-of-the-art baselines and outperforming other optimization methods. This remarkable achievement motivates researchers and practitioners to explore new approaches for further improving machine learning models and pushes the boundaries of what is achievable in model performance. From an ethical standpoint, SEMA as a regularization technique does not raise any concerns. It adheres to established ethical guidelines and principles, focusing solely on improving model performance through regularization. It does not involve collecting or using sensitive data, ensuring fairness and transparency in its application. SEMA’s ethical considerations make it a responsible and valuable tool for advancing machine learning without introducing biases or discriminatory practices.

References

- Yelp dataset challenge. http://www.yelp.com/dataset_challenge.
- Andriushchenko, M., D’Angelo, F., Varre, A., and Flammarion, N. Why do we need weight decay in modern deep learning? *ArXiv*, abs/2310.04415, 2023.
- Bishop, C. M. *Pattern recognition and machine learning*. springer, 2006.
- Cai, Z. and Vasconcelos, N. Cascade r-cnn: High-quality object detection and instance segmentation. *IEEE Transactions on Pattern Analysis and Machine Intelligence*, 2019. ISSN 1939-3539.
- Chen, K., Wang, J., Pang, J., Cao, Y., Xiong, Y., Li, X., Sun, S., Feng, W., Liu, Z., Xu, J., Zhang, Z., Cheng, D., Zhu, C., Cheng, T., Zhao, Q., Li, B., Lu, X., Zhu, R., Wu, Y., Dai, J., Wang, J., Shi, J., Ouyang, W., Loy, C. C., and Lin, D. MMDetection: Open mmlab detection toolbox and benchmark. <https://github.com/open-mmlab/mmdetection>, 2019.
- Chen, T., Kornblith, S., Norouzi, M., and Hinton, G. A simple framework for contrastive learning of visual representations. In *International Conference on Machine Learning (ICML)*, 2020a.
- Chen, X., Fan, H., Girshick, R., and He, K. Improved baselines with momentum contrastive learning. *arXiv preprint arXiv:2003.04297*, 2020b.
- Chen, X., Xie, S., and He, K. An empirical study of training self-supervised vision transformers. In *International Conference on Computer Vision (ICCV)*, pp. 9640–9649, 2021.
- Chen, Y., Dai, X., Chen, D., Liu, M., Dong, X., Yuan, L., and Liu, Z. Mobile-former: Bridging mobilenet and transformer. In *Conference on Computer Vision and Pattern Recognition (CVPR)*, 2022.
- Coates, A., Ng, A., and Lee, H. An analysis of single-layer networks in unsupervised feature learning. In Gordon, G., Dunson, D., and Dudík, M. (eds.), *Proceedings of the Fourteenth International Conference on Artificial Intelligence and Statistics*, volume 15 of *Proceedings of Machine Learning Research*, pp. 215–223, Fort Lauderdale, FL, USA, 11–13 Apr 2011. PMLR.
- Cubuk, E. D., Zoph, B., Mané, D., Vasudevan, V., and Le, Q. V. Autoaugment: Learning augmentation strategies from data. *Conference on Computer Vision and Pattern Recognition (CVPR)*, pp. 113–123, 2019.
- Cubuk, E. D., Zoph, B., Shlens, J., and Le, Q. V. Randaugment: Practical automated data augmentation with a reduced search space. In *Proceedings of the IEEE/CVF Conference on Computer Vision and Pattern Recognition Workshops (CVPRW)*, pp. 702–703, 2020.
- Deng, J., Dong, W., Socher, R., Li, L.-J., Li, K., and Fei-Fei, L. ImageNet: A large-scale hierarchical image database. In *Conference on Computer Vision and Pattern Recognition (CVPR)*, 2009.
- Devlin, J., Chang, M.-W., Lee, K., and Toutanova, K. Bert: Pre-training of deep bidirectional transformers for language understanding. *arXiv:1810.04805*, 2018.

- DeVries, T. and Taylor, G. W. Improved regularization of convolutional neural networks with cutout, 2017.
- Dosovitskiy, A., Beyer, L., Kolesnikov, A., Weissenborn, D., Zhai, X., Unterthiner, T., Dehghani, M., Minderer, M., Heigold, G., Gelly, S., et al. An image is worth 16x16 words: Transformers for image recognition at scale. In *International Conference on Learning Representations (ICLR)*, 2020.
- Du, J., Yan, H., Feng, J., Zhou, J. T., Zhen, L., Goh, R. S. M., and Tan, V. Y. F. Efficient sharpness-aware minimization for improved training of neural networks. In *International Conference on Learning Representations (ICLR)*, 2021.
- Du, J., Zhou, D., Feng, J., Tan, V. Y. F., and Zhou, J. T. Sharpness-aware training for free. In *Advances in Neural Information Processing Systems (NeurIPS)*, 2022.
- Foret, P., Kleiner, A., Mobahi, H., and Neyshabur, B. Sharpness-aware minimization for efficiently improving generalization. In *International Conference on Learning Representations*, 2021.
- Gao, Z., Tan, C., Wu, L., and Li, S. Z. Simvp: Simpler yet better video prediction. In *Conference on Computer Vision and Pattern Recognition (CVPR)*, pp. 3170–3180, June 2022.
- Garipov, T., Izmailov, P., Podoprikin, D., Vetrov, D. P., and Wilson, A. G. Loss surfaces, mode connectivity, and fast ensembling of dnns. In *Advances in Neural Information Processing Systems*, volume 31. Curran Associates, Inc., 2018.
- Ge, Z., Liu, S., Wang, F., Li, Z., and Sun, J. YoloX: Exceeding yolo series in 2021. *ArXiv*, abs/2107.08430, 2021.
- Ginsburg, B., Gitman, I., and You, Y. Large batch training of convolutional networks with layer-wise adaptive rate scaling. In *International Conference on Learning Representations (ICLR)*, 2018.
- Goodfellow, I. J., Vinyals, O., and Saxe, A. M. Qualitatively characterizing neural network optimization problems, 2015.
- Granzio, D., Wan, X., Albanie, S., and Roberts, S. Iterative averaging in the quest for best test error, 2021.
- Grill, J.-B., Strub, F., Altché, F., Tallec, C., Richemond, P. H., Buchatskaya, E., Doersch, C., Pires, B. A., Guo, Z. D., Azar, M. G., et al. Bootstrap your own latent: A new approach to self-supervised learning. In *Advances in Neural Information Processing Systems (NeurIPS)*, 2020.
- Guo, H., Jin, J., and Liu, B. Stochastic weight averaging revisited, 2022.
- Guo, H., Jin, J., and Liu, B. Pfge: Parsimonious fast geometric ensembling of dnns, 2023.
- He, K., Zhang, X., Ren, S., and Sun, J. Deep residual learning for image recognition. In *Conference on Computer Vision and Pattern Recognition (CVPR)*, pp. 770–778, 2016.
- He, K., Gkioxari, G., Dollár, P., and Girshick, R. Mask r-cnn. In *International Conference on Computer Vision (ICCV)*, 2017.
- He, K., Fan, H., Wu, Y., Xie, S., and Girshick, R. Momentum contrast for unsupervised visual representation learning. In *Conference on Computer Vision and Pattern Recognition (CVPR)*, pp. 9729–9738, 2020.
- He, K., Chen, X., Xie, S., Li, Y., Dollár, P., and Girshick, R. Masked autoencoders are scalable vision learners. In *Conference on Computer Vision and Pattern Recognition (CVPR)*, 2022.
- He, W., Li, B., and Song, D. Decision boundary analysis of adversarial examples. In *International Conference on Learning Representations*, 2018. URL <https://openreview.net/forum?id=BkpiPMbA->.
- Ho, J., Jain, A., and Abbeel, P. Denoising diffusion probabilistic models. In Larochelle, H., Ranzato, M., Hadsell, R., Balcan, M., and Lin, H. (eds.), *Advances in Neural Information Processing Systems*, volume 33, pp. 6840–6851. Curran Associates, Inc., 2020.
- Huang, G., Sun, Y., Liu, Z., Sedra, D., and Weinberger, K. Q. Deep networks with stochastic depth. In *European Conference on Computer Vision (ECCV)*, 2016.
- Huang, G., Liu, Z., and Weinberger, K. Q. Densely connected convolutional networks. In *Conference on Computer Vision and Pattern Recognition (CVPR)*, pp. 2261–2269, 2017.
- Izmailov, P., Podoprikin, D., Garipov, T., Vetrov, D., and Wilson, A. Averaging weights leads to wider optima and better generalization. In Silva, R., Globerson, A., and Globerson, A. (eds.), *34th Conference on Uncertainty in Artificial Intelligence 2018, UAI 2018*, 34th Conference on Uncertainty in Artificial Intelligence 2018, UAI 2018, pp. 876–885. Association For Uncertainty in Artificial Intelligence (AUAI), 2018.
- Kaddour, J. Stop wasting my time! saving days of imagenet and bert training with latest weight averaging, 2022.
- Kaddour, J., Liu, L., Silva, R. M. A., and Kusner, M. J. When do flat minima optimizers work? In *Neural Information Processing Systems*, 2022.

- Karras, T., Aittala, M., Lehtinen, J., Hellsten, J., Aila, T., and Laine, S. Analyzing and improving the training dynamics of diffusion models. *ArXiv*, abs/2312.02696, 2023.
- Kingma, D. P. and Ba, J. Adam: A method for stochastic optimization. In *International Conference on Learning Representations (ICLR)*, 2014.
- Kobayashi, T. Scw-sgd: Stochastically confidence-weighted sgd. *2020 IEEE International Conference on Image Processing (ICIP)*, pp. 1746–1750, 2020.
- Krizhevsky, A., Hinton, G., et al. Learning multiple layers of features from tiny images. 2009.
- Krizhevsky, A., Sutskever, I., and Hinton, G. E. Imagenet classification with deep convolutional neural networks. *Communications of the ACM*, 60:84 – 90, 2012.
- Li, H., Xu, Z., Taylor, G., and Goldstein, T. Visualizing the loss landscape of neural nets. *CoRR*, abs/1712.09913, 2017.
- Li, H., Xu, Z., Taylor, G., Studer, C., and Goldstein, T. Visualizing the loss landscape of neural nets. *Advances in neural information processing systems*, 31, 2018.
- Li, S., Liu, Z., Wang, Z., Wu, D., Liu, Z., and Li, S. Z. Boosting discriminative visual representation learning with scenario-agnostic mixup. *ArXiv*, abs/2111.15454, 2021.
- Li, S., Wang, Z., Liu, Z., Wu, D., and Li, S. Z. Openmixup: Open mixup toolbox and benchmark for visual representation learning. <https://github.com/Westlake-AI/openmixup>, 2022.
- Li, S., Wu, D., Wu, F., Zang, Z., and Stan.Z.Li. Architecture-agnostic masked image modeling - from vit back to cnn. In *International Conference on Machine Learning (ICML)*, 2023a.
- Li, S., Jin, W., Wang, Z., Wu, F., Liu, Z., Tan, C., and Li, S. Z. Semireward: A general reward model for semi-supervised learning. In *International Conference on Learning Representations*, 2024a.
- Li, S., Wang, Z., Liu, Z., Tan, C., Lin, H., Wu, D., Chen, Z., Zheng, J., and Li, S. Z. Efficient multi-order gated aggregation network. In *International Conference on Learning Representations*, 2024b.
- Li, T., Huang, Z., Wu, Y., He, Z., Tao, Q., Huang, X., and Lin, C.-J. Trainable weight averaging: A general approach for subspace training. In *International Conference on Learning Representations (ICLR)*, 2023b.
- Lin, T.-Y., Maire, M., Belongie, S., Hays, J., Perona, P., Ramanan, D., Dollár, P., and Zitnick, C. L. Microsoft coco: Common objects in context. In *European Conference on Computer Vision (ECCV)*, pp. 740–755. Springer, 2014.
- Lin, T.-Y., Goyal, P., Girshick, R., He, K., and Dollár, P. Focal loss for dense object detection. In *International Conference on Computer Vision (ICCV)*, 2017.
- Liu, L., Jiang, H., He, P., Chen, W., Liu, X., Gao, J., and Han, J. On the variance of the adaptive learning rate and beyond. In *International Conference on Learning Representations*, 2020.
- Liu, Y., Mai, S., Chen, X., Hsieh, C.-J., and You, Y. Towards efficient and scalable sharpness-aware minimization. In *Conference on Computer Vision and Pattern Recognition (CVPR)*, pp. 12350–12360, 2022a.
- Liu, Z., Luo, P., Wang, X., and Tang, X. Deep learning face attributes in the wild. In *Proceedings of International Conference on Computer Vision (ICCV)*, December 2015.
- Liu, Z., Lin, Y., Cao, Y., Hu, H., Wei, Y., Zhang, Z., Lin, S., and Guo, B. Swin transformer: Hierarchical vision transformer using shifted windows. In *International Conference on Computer Vision (ICCV)*, 2021.
- Liu, Z., Li, S., Wang, G., Tan, C., Wu, L., and Li, S. Z. Decoupled mixup for data-efficient learning. *ArXiv*, abs/2203.10761, 2022b.
- Liu, Z., Li, S., Wu, D., Chen, Z., Wu, L., Guo, J., and Li, S. Z. Automix: Unveiling the power of mixup for stronger classifiers. In *European Conference on Computer Vision (ECCV)*, 2022c.
- Liu, Z., Mao, H., Wu, C.-Y., Feichtenhofer, C., Darrell, T., and Xie, S. A convnet for the 2020s. In *Conference on Computer Vision and Pattern Recognition (CVPR)*, pp. 11976–11986, 2022d.
- Loshchilov, I. and Hutter, F. Decoupled weight decay regularization. In *International Conference on Learning Representations (ICLR)*, 2019.
- Ma, X., Tao, Z., Wang, Y., Yu, H., and Wang, Y. Long short-term memory neural network for traffic speed prediction using remote microwave sensor data. *Transportation Research Part C: Emerging Technologies*, 54:187–197, 2015. ISSN 0968-090X. doi: <https://doi.org/10.1016/j.trc.2015.03.014>.
- Maddox, W. J., Garipov, T., Izmailov, P., Vetrov, D. P., and Wilson, A. G. A simple baseline for bayesian uncertainty in deep learning. In *Advances in Neural Information Processing Systems (NeurIPS)*, volume 32, 2019.

- Marcus, M. P., Marcinkiewicz, M. A., and Santorini, B. Building a large annotated corpus of english: the penn treebank. *Comput. Linguist.*, 19(2):313–330, jun 1993. ISSN 0891-2017.
- Mehta, S. and Rastegari, M. Mobilevit: light-weight, general-purpose, and mobile-friendly vision transformer. In *International Conference on Learning Representations (ICLR)*, 2022.
- Mnih, V., Badia, A. P., Mirza, M., Graves, A., Harley, T., Lillicrap, T. P., Silver, D., and Kavukcuoglu, K. Asynchronous methods for deep reinforcement learning. In *Proceedings of the 33rd International Conference on International Conference on Machine Learning - Volume 48*, ICML’16, pp. 1928–1937. JMLR.org, 2016.
- Moschoglou, S., Papaioannou, A., Sagonas, C., Deng, J., Kotsia, I., and Zafeiriou, S. Agedb: The first manually collected, in-the-wild age database. In *Proceedings of the IEEE Conference on Computer Vision and Pattern Recognition (CVPR) Workshops*, July 2017.
- Ott, M., Edunov, S., Baevski, A., Fan, A., Gross, S., Ng, N., Grangier, D., and Auli, M. fairseq: A fast, extensible toolkit for sequence modeling. In Ammar, W., Louis, A., and Mostafazadeh, N. (eds.), *Proceedings of the 2019 Conference of the North American Chapter of the Association for Computational Linguistics (Demonstrations)*, pp. 48–53, Minneapolis, Minnesota, June 2019. Association for Computational Linguistics. doi: 10.18653/v1/N19-4009.
- Pedregosa, F., Varoquaux, G., Gramfort, A., Michel, V., Thirion, B., Grisel, O., Blondel, M., Prettenhofer, P., Weiss, R., Dubourg, V., Vanderplas, J., Passos, A., Cournapeau, D., Brucher, M., Perrot, M., and Duchesnay, E. Scikit-learn: Machine learning in Python. *Journal of Machine Learning Research*, 12:2825–2830, 2011.
- Peng, C., Xiao, T., Li, Z., Jiang, Y., Zhang, X., Jia, K., Yu, G., and Sun, J. Megdet: A large mini-batch object detector. In *Conference on Computer Vision and Pattern Recognition (CVPR)*, pp. 6181–6189, 2018.
- Polyak, B. and Juditsky, A. B. Acceleration of stochastic approximation by averaging. *Siam Journal on Control and Optimization*, 30:838–855, 1992.
- Rothe, R., Timofte, R., and Van Gool, L. Deep expectation of real and apparent age from a single image without facial landmarks. *Int. J. Comput. Vision*, 126(2–4):144–157, apr 2018. ISSN 0920-5691.
- Rumelhart, D. E., Hinton, G. E., and Williams, R. J. *Learning internal representations by error propagation*, pp. 318–362. MIT Press, Cambridge, MA, USA, 1986. ISBN 026268053X.
- Shi, X., Chen, Z., Wang, H., Yeung, D.-Y., Wong, W.-K., and Woo, W.-c. Convolutional lstm network: A machine learning approach for precipitation nowcasting. *Advances in Neural Information Processing Systems*, 28, 2015.
- Simonyan, K. and Zisserman, A. Very deep convolutional networks for large-scale image recognition. *arXiv preprint arXiv:1409.1556*, 2014.
- Sinha, N. K. and Griscik, M. P. A stochastic approximation method. *IEEE Transactions on Systems, Man, and Cybernetics*, SMC-1(4):338–344, Oct 1971.
- Sohn, K., Berthelot, D., Li, C.-L., Zhang, Z., Carlini, N., Cubuk, E. D., Kurakin, A., Zhang, H., and Raffel, C. Fixmatch: Simplifying semi-supervised learning with consistency and confidence. In *Advances in Neural Information Processing Systems (NeurIPS)*, 2020.
- Song, J., Meng, C., and Ermon, S. Denoising diffusion implicit models. In *International Conference on Learning Representations*, 2021.
- Srivastava, N., Hinton, G., Krizhevsky, A., Sutskever, I., and Salakhutdinov, R. Dropout: a simple way to prevent neural networks from overfitting. *J. Mach. Learn. Res.*, 15(1):1929–1958, jan 2014. ISSN 1532-4435.
- Srivastava, N., Mansimov, E., and Salakhutdinov, R. Unsupervised learning of video representations using LSTMs. In *International Conference on Machine Learning (ICML)*, 2015.
- Sutskever, I., Martens, J., Dahl, G., and Hinton, G. On the importance of initialization and momentum in deep learning. In *Proceedings of the 30th International Conference on International Conference on Machine Learning - Volume 28*, ICML’13, pp. III–1139–III–1147. JMLR.org, 2013.
- Szegedy, C., Liu, W., Jia, Y., Sermanet, P., Reed, S., Anguelov, D., Erhan, D., Vanhoucke, V., and Rabinovich, A. Going deeper with convolutions. In *Conference on Computer Vision and Pattern Recognition (CVPR)*, pp. 1–9, 2015.
- Szegedy, C., Vanhoucke, V., Ioffe, S., Shlens, J., and Wojna, Z. Rethinking the inception architecture for computer vision. *Conference on Computer Vision and Pattern Recognition (CVPR)*, pp. 2818–2826, 2016.
- Tan, C., Li, S., Gao, Z., Guan, W., Wang, Z., Liu, Z., Wu, L., and Li, S. Z. Openstl: A comprehensive benchmark of spatio-temporal predictive learning. In *Conference on Neural Information Processing Systems Datasets and Benchmarks Track*, 2023.

- Tolstikhin, I. O., Houlsby, N., Kolesnikov, A., Beyer, L., Zhai, X., Unterthiner, T., Yung, J., Keysers, D., Uszkoreit, J., Lucic, M., and Dosovitskiy, A. Mlp-mixer: An all-mlp architecture for vision. In *Advances in Neural Information Processing Systems (NeurIPS)*, 2021.
- Touvron, H., Cord, M., Douze, M., Massa, F., Sablayrolles, A., and Jegou, H. Training data-efficient image transformers & distillation through attention. In *International Conference on Machine Learning (ICML)*, pp. 10347–10357, 2021.
- Wang, Y., Long, M., Wang, J., Gao, Z., and Yu, P. S. Predrnn: Recurrent neural networks for predictive learning using spatiotemporal lstms. *Advances in Neural Information Processing Systems*, 30, 2017.
- Wang, Y., Chen, H., Fan, Y., SUN, W., Tao, R., Hou, W., Wang, R., Yang, L., Zhou, Z., Guo, L.-Z., Qi, H., Wu, Z., Li, Y.-F., Nakamura, S., Ye, W., Savvides, M., Raj, B., Shinozaki, T., Schiele, B., Wang, J., Xie, X., and Zhang, Y. Usb: A unified semi-supervised learning benchmark for classification. In Koyejo, S., Mohamed, S., Agarwal, A., Belgrave, D., Cho, K., and Oh, A. (eds.), *Advances in Neural Information Processing Systems*, volume 35, pp. 3938–3961. Curran Associates, Inc., 2022.
- Wightman, R., Touvron, H., and Jégou, H. Resnet strikes back: An improved training procedure in timm. <https://github.com/huggingface/pytorch-image-models>, 2021.
- Wortsman, M., Ilharco, G., Gadre, S. Y., Roelofs, R., Lopes, R. G., Morcos, A. S., Namkoong, H., Farhadi, A., Carmon, Y., Kornblith, S., and Schmidt, L. Model soups: averaging weights of multiple fine-tuned models improves accuracy without increasing inference time. In *International Conference on Machine Learning (ICML)*, pp. 23965–23998, 2022.
- Wright, L. Ranger - a synergistic optimizer. <https://github.com/lessw2020/Ranger-Deep-Learning-Optimizer>, 2019.
- Wu, Y. and Johnson, J. Rethinking "batch" in batchnorm. *ArXiv*, abs/2105.07576, 2021.
- Xie, S., Girshick, R., Dollár, P., Tu, Z., and He, K. Aggregated residual transformations for deep neural networks. In *Conference on Computer Vision and Pattern Recognition (CVPR)*, pp. 1492–1500, 2017.
- Xie, X., Zhou, P., Li, H., Lin, Z., and YAN, S. Adan: Adaptive nesterov momentum algorithm for faster optimizing deep models. *IEEE Transactions on Pattern Analysis and Machine Intelligence*, 2023.
- Xie, Z., Zhang, Z., Cao, Y., Lin, Y., Bao, J., Yao, Z., Dai, Q., and Hu, H. Simmim: A simple framework for masked image modeling. In *Conference on Computer Vision and Pattern Recognition (CVPR)*, 2022.
- Yao, H., Wang, Y., Zhang, L., Zou, J. Y., and Finn, C. C-mixup: Improving generalization in regression. In Koyejo, S., Mohamed, S., Agarwal, A., Belgrave, D., Cho, K., and Oh, A. (eds.), *Advances in Neural Information Processing Systems*, volume 35, pp. 3361–3376. Curran Associates, Inc., 2022.
- You, Y., Li, J., Reddi, S., Hseu, J., Kumar, S., Bhojanapalli, S., Song, X., Demmel, J., Keutzer, K., and Hsieh, C.-J. Large batch optimization for deep learning: Training BERT in 76 minutes. In *International Conference on Learning Representations (ICLR)*, 2020.
- Yu, W., Luo, M., Zhou, P., Si, C., Zhou, Y., Wang, X., Feng, J., and Yan, S. Metaformer is actually what you need for vision. In *Conference on Computer Vision and Pattern Recognition (CVPR)*, pp. 10819–10829, 2022.
- Yun, S., Han, D., Oh, S. J., Chun, S., Choe, J., and Yoo, Y. Cutmix: Regularization strategy to train strong classifiers with localizable features. In *International Conference on Computer Vision (ICCV)*, pp. 6023–6032, 2019.
- Zagoruyko, S. and Komodakis, N. Wide residual networks. In *Proceedings of the British Machine Vision Conference (BMVC)*, 2016.
- Zbontar, J., Jing, L., Misra, I., LeCun, Y., and Deny, S. Barlow twins: Self-supervised learning via redundancy reduction. In *International Conference on Machine Learning (ICML)*, pp. 12310–12320. PMLR, 2021.
- Zhang, H., Cisse, M., Dauphin, Y. N., and Lopez-Paz, D. mixup: Beyond empirical risk minimization. In *International Conference on Learning Representations (ICLR)*, 2018.
- Zhang, H., Wang, Y., Dayoub, F., and Sunderhauf, N. Swa object detection. *ArXiv*, abs/2012.12645, 2020.
- Zhang, H., Hu, W., and Wang, X. Edgeformer: Improving light-weight convnets by learning from vision transformers. In *European Conference on Computer Vision (ECCV)*, 2022.
- Zhang, M., Lucas, J., Ba, J., and Hinton, G. E. Lookahead optimizer: k steps forward, 1 step back. In *Advances in Neural Information Processing Systems*, volume 32. Curran Associates, Inc., 2019.
- Zhong, Z., Zheng, L., Kang, G., Li, S., and Yang, Y. Random erasing data augmentation. In *AAAI*, pp. 13001–13008, 2020.

Zhou, P., Yan, H., Yuan, X., Feng, J., and Yan, S. Towards understanding why lookahead generalizes better than sgd and beyond. In Ranzato, M., Beygelzimer, A., Dauphin, Y., Liang, P., and Vaughan, J. W. (eds.), *Advances in Neural Information Processing Systems*, volume 34, pp. 27290–27304. Curran Associates, Inc., 2021.

Zhuang, J., Tang, T., Ding, Y., Tatikonda, S. C., Dvornek, N., Papademetris, X., and Duncan, J. Adabelief optimizer: Adapting stepsizes by the belief in observed gradients. In Larochelle, H., Ranzato, M., Hadsell, R., Balcan, M., and Lin, H. (eds.), *Advances in Neural Information Processing Systems*, volume 33, pp. 18795–18806. Curran Associates, Inc., 2020.

Zhuang, J., Gong, B., Yuan, L., Cui, Y., Adam, H., Dvornek, N. C., Tatikonda, S. C., Duncan, J. S., and Liu, T. Surrogate gap minimization improves sharpness-aware training. In *International Conference on Learning Representations (ICLR)*, 2022.

A. Proof of Proposition

Taking SGD as an example, we provide two propositions and their proofs of SEMA to investigate the favorable properties mentioned in Sec. 3.2 and Sec. 3.3. Let η be the learning rate of the optimizer and λ be the decay rate of SGD, EMA, and SEMA. In the noise quadratic model, the loss of iterates Θ_t is defined as:

$$\mathcal{L}(\Theta_t) = \frac{1}{2}(\Theta_t - c)^T A(\Theta_t - c),$$

where $c \sim \mathcal{N}(\theta^*, \Sigma)$. Without loss of generality, we set $\theta^* = 0$. Then, we can define the iterates of SGD, EMA, and SEMA (denoted as θ_t , $\tilde{\theta}_t$ and θ_t^* respectively) as follows:

$$\begin{aligned}\theta_t &= \theta_{t-1} - \eta \nabla \mathcal{L}(\theta_{t-1}), \\ \tilde{\theta}_t &= \lambda \theta_t + (1 - \lambda) \tilde{\theta}_{t-1}, \\ \theta_t' &= \theta_{t-1}^* - \eta \nabla \mathcal{L}(\theta_{t-1}^*), \\ \theta_t^* &= \lambda \theta_t' + (1 - \lambda) \theta_{t-1}^*, \\ \theta_0 &= \tilde{\theta}_0 = \theta_0^*.\end{aligned}$$

Notice that iterates of θ_t and $\tilde{\theta}_t$ are defined jointly, and θ_t' is an intermediate iterate assisting to define the iterate of θ_t^* .

A.1. Proof of Proposition 1

Proposition 1. low-frequency oscillation: In the noisy quadratic model, the variance of SGD, EMA, and SEMA iterates, denoted as V_{SGD} , V_{EMA} and V_{SEMA} respectively, converge to following fixed points, *i.e.*, $V_{\text{SEMA}} < V_{\text{EMA}} < V_{\text{SGD}}$:

$$\begin{aligned}V_{\text{SGD}} &= \frac{\eta A}{2I - \eta A} \Sigma, \\ V_{\text{EMA}} &= \frac{\lambda}{2 - \lambda} \cdot \frac{2 - \lambda - (1 - \lambda)\eta A}{\lambda + (1 - \lambda)\eta A} \cdot V_{\text{SGD}}, \\ V_{\text{SEMA}} &= \frac{2 - \lambda}{\lambda} \cdot \frac{\lambda + (1 - \lambda)\eta A}{2 - \lambda - (1 - \lambda)\eta A} \cdot \frac{\lambda \eta A}{2I - \lambda \eta A} \cdot \frac{2I - \eta A}{\eta A} \cdot V_{\text{EMA}}.\end{aligned}$$

Proof. First, we compute the stochastic dynamics of SGD, EMA, and SEMA. According to the property of variance and quadratic loss, we can get stochastic variance dynamics from iterates of trajectories:

$$\begin{aligned}V(\theta_t) &= (I - \eta A)^2 V(\theta_{t-1}) + \eta^2 A^2 \Sigma, \\ V(\tilde{\theta}_t) &= \lambda^2 V(\theta_t) + (1 - \lambda)^2 V(\tilde{\theta}_{t-1}) + 2\lambda(1 - \lambda) \text{Cov}(\theta_t, \tilde{\theta}_{t-1}), \\ \text{Cov}(\theta_t, \tilde{\theta}_{t-1}) &= \lambda(I - \eta A)V(\theta_{t-1}) + (1 - \lambda)(I - \eta A)\text{Cov}(\theta_{t-1}, \tilde{\theta}_{t-2}), \\ V(\theta_t^*) &= (I - \lambda \eta A)^2 V(\theta_{t-1}^*) + \lambda^2 \eta^2 A^2 \Sigma.\end{aligned}$$

Then, using Banach's fixed point theorem, we can easily derive V_{SGD} , V_{EMA} and V_{SEMA} as follows:

$$\begin{aligned}V_{\text{SGD}} &= (I - \eta A)^2 V_{\text{SGD}} + \eta^2 A^2 \Sigma, \\ V_{\text{SGD}} &= \frac{\eta A}{2I - \eta A} \Sigma, \\ V_{\text{EMA}} &= \lambda^2 V_{\text{SGD}} + (1 - \lambda)^2 V_{\text{EMA}} + 2\lambda(1 - \lambda) \text{Cov}(\text{SGD}, \text{EMA}), \\ \text{Cov}(\text{SGD}, \text{EMA}) &= \lambda(I - \eta A)V_{\text{SGD}} + (1 - \lambda)(I - \eta A)\text{Cov}(\text{SGD}, \text{EMA}), \\ V_{\text{EMA}} &= \frac{\lambda}{2 - \lambda} \cdot \frac{2 - \lambda - (1 - \lambda)\eta A}{\lambda + (1 - \lambda)\eta A} \cdot V_{\text{SGD}}, \\ V_{\text{SEMA}} &= (I - \lambda \eta A)^2 V_{\text{SEMA}} + \lambda^2 \eta^2 A^2 \Sigma, \\ V_{\text{SEMA}} &= \frac{\lambda \eta A}{2I - \lambda \eta A} \Sigma.\end{aligned}$$

Finally, we will prove inequality $V_{\text{SEMA}} < V_{\text{EMA}} < V_{\text{SGD}}$. To prove this, we only need to show the following two coefficients less or equal to one:

$$\begin{aligned}\text{coef}_1 &= \frac{\lambda}{2-\lambda} \cdot \frac{2-\lambda-(1-\lambda)\eta A}{\lambda+(1-\lambda)\eta A}, \\ \text{coef}_2 &= \frac{2-\lambda}{\lambda} \cdot \frac{\lambda+(1-\lambda)\eta A}{2-\lambda-(1-\lambda)\eta A} \cdot \frac{\lambda\eta A}{2I-\lambda\eta A} \cdot \frac{2I-\eta A}{\eta A}.\end{aligned}$$

For coef_1 , we can see it is a decreasing function w.r.t η , and $\text{coef}_1 = 1$ when $\eta = 0$. Thus for $\eta > 0$, $\text{coef}_1 < 1$. For coef_2 , we can simplify it as following:

$$\text{coef}_2 = \frac{\lambda+(1-\lambda)\eta A}{1-\frac{1-\lambda}{2-\lambda}\eta A} \cdot \frac{2I-\eta A}{2I-\lambda\eta A}.$$

Because learning rate η and decay rate λ are both quite small numbers, one can easily show that these two terms are smaller than 1, thus $\text{coef}_2 < 1$.

A.2. Proof of Proposition 2

Proposition 2. fast convergence: The iteration of SEMA ensures the gradient descent property, which SGD has but EMA doesn't have. More specifically expressed as:

$$(\theta_{t+1}^* - \theta_t^*) \propto -\nabla \mathcal{L}(\theta_{\square}).$$

Proof. This property is easily obtained by putting $\theta'_t = \theta_{t-1}^* - \eta \nabla \mathcal{L}(\theta_{\square-\infty}^*)$ into $\theta_t^* = \lambda \theta'_t + (1-\lambda)\theta_{t-1}^*$, then we have:

$$\theta_t^* = \theta_{t-1}^* - \lambda \eta \nabla \mathcal{L}(\theta_{\square-\infty}^*).$$

Integrated Analysis. As substantiated by *Propositions* above and the evidence in Figure 4, SEMA converges significantly faster to a local optimum than EMA does because of its effective amalgamation of the gradient descent characteristics of the baseline model and the stability advantage of EMA. The optimization process of SEMA will be efficiently steered towards local minima unimpeded by slow or irregular parameter updates. In contrast, EMA lacks this benefit, potentially leading to it being ensnared in a flat but inferior local basin.

B. Implementation Details

This section provides implementation settings and dataset information for empirical experiments conducted in Sec. 4. We follow existing benchmarks for all experiments to ensure fair comparisons. As for the compared WA methods and Lookahead, we adopt the following settings: EMA is applied as test-time regularization during the whole training process with tuned momentum coefficient; SWA applies the 1.25 budget (e.g., ensemble five models iteratively); Lookahead applies the slow model learning rate with $\alpha = 0.5$ and the update interval $k = 100$. Meanwhile, SEMA uses “by-epoch” switching, (i.e., T is the iteration number of traversing the entire training set once, and the momentum ratios for different tasks are shown in Table A1 and Table A2.

B.1. Image classification

We evaluate WA methods with image classification tasks based on various optimizers and network architectures on CIFAR-100 (Krizhevsky et al., 2009) and ImageNet-1K (Deng et al., 2009). Experiments are implemented on OpenMixup (Li et al., 2022) codebase with 1 or 8 Nvidia A100 GPUs.

ImageNet-1K. We perform regular ImageNet-1K classification experiments following the widely used training settings with various optimizers and backbone architectures, as shown in Table A3. We consider popular backbone models, including ResNet (He et al., 2016), DeiT (Vision Transformer) (Dosovitskiy et al., 2020; Touvron et al., 2021), Swin Transformer (Liu et al., 2021), ConvNeXt (Liu et al., 2022d), and MogaNet (Li et al., 2024b). For all models, the default input image resolution is 224^2 for training from scratch on 1.28M training images and testing on 50k validation images. ConvNeXt and Swin share the same training settings. As for augmentation and regularization techniques, we adopt most of the data augmentation and regularization strategies applied in DeiT training settings, including Random Resized Crop (RRC) and Horizontal flip (Szegedy et al., 2015), RandAugment (Cubuk et al., 2020), Mixup (Zhang et al., 2018), CutMix (Yun et al., 2019), random erasing (Zhong et al., 2020), ColorJitter (He et al., 2016), stochastic depth (Huang et al., 2016), and label smoothing (Szegedy et al., 2016). Note that EMA (Polyak & Juditsky, 1992) with the momentum coefficient of 0.9999 is basically adopted in DeiT and ConvNeXt training, but remove it as the baseline in Table 2. We also remove additional augmentation strategies (Cubuk et al., 2019; Liu et al., 2022c; Li et al., 2021; Liu et al., 2022b), e.g., PCA lighting (Krizhevsky et al., 2012) and AutoAugment (Cubuk et al., 2019). Since lightweight architectures (3~10M parameters) tend to get under-fitted with strong augmentations and regularization, we adjust the training configurations for MogaNet-XT/T following (Mehta & Rastegari, 2022; Chen

et al., 2022; Zhang et al., 2022), including employing the weight decay of 0.03 and 0.04, Mixup with α of 0.1, and RandAugment of 7/0.5 for MogaNet-XT/T. Since EMA is proposed to stabilize the training process of large models, we also remove it for MogaNet-XT/T as a fair comparison. An increasing degree of stochastic depth path augmentation is employed for larger models. In evaluation, the top-1 accuracy using a single crop with a test crop ratio of 0.85 is reported by default.

CIFAR-100. We use different training settings for a fair comparison of classical CNNs and modern Transformers on CIFAR-100, which contains 50k training images and 10k testing images of 32^2 resolutions. As for classical CNNs with bottleneck structures, including ResNet variants, ResNeXt (Xie et al., 2017), Wide-ResNet (Zagoruyko & Komodakis, 2016), and DenseNet (Huang et al., 2017), we use 32^2 resolutions with the CIFAR version of network architectures, i.e., downsampling the input size to $\frac{1}{2}$ in the stem module instead of $\frac{1}{8}$ on ImageNet-1K. Meanwhile, we train three modern architectures for 200 epochs from the stretch. We resize the raw images to 224^2 resolutions for DeiT-S and Swin-T while modifying the stem network as the CIFAR version of ResNet for ConvNeXt-T with 32^2 resolutions.

B.2. Self-supervised Learning

We consider two categories of popular self-supervised learning (SSL) on CIFAR-100, STL-10 (Coates et al., 2011), and ImageNet-1K: contrastive learning (CL) for discriminative representation and masked image modeling (MIM) for more generalizable representation. Experiments are implemented on OpenMixup codebase with 4 Tesla V100 GPUs.

Contrastive Learning. To verify the effectiveness of WA methods with CL methods with both self-teaching or non-teaching frameworks, we evaluate five classical CL methods on CIFAR-100, STL-10, and ImageNet-1K datasets, including SimCLR (Chen et al., 2020a), MoCo.V2 (Chen et al., 2020b), BYOL (Grill et al., 2020), Barlow Twins (Zbontar et al., 2021), and MoCo.V3 (Chen et al., 2020b). STL-10 is a widely used dataset for SSL or semi-supervised tasks, consisting of 5K labeled training images for 10 classes and 100K unlabelled training images, and a test set of 8K images in 96^2 resolutions. The pre-training settings are borrowed from their original papers on ImageNet-1K, as shown in Table A4. As for the SimCLR augmentations, the recipes include *RandomResizedCrop* with the scale in $[0.08, 1.0]$ and *RandomHorizontalFlip*, color augmentations of *ColorJitter* with {brightness, contrast, saturation, hue} strength of $\{0.4, 0.4, 0.4, 0.1\}$ with an applying probability of 0.8 and *RandomGrayscale* with an applying probability of 0.2, and blurring augmentations of a Gaussian kernel of size

Table A1: Momentum coefficient α in EMA and SEMA for vision applications, including image classification (Cls.), self-supervised learning (SSL) with contrastive learning (CL) methods or masked image modeling (MIM) methods, objection detection (Det.) and instance segmentation (Seg.), and image generation (Gen.) tasks.

Dataset	CIFAR-100			STL-10		ImageNet-1K			CIFAR-10	CelebA	COCO	
Task	Cls.	SSL (CL)	SSL (MIM)	SSL (CL)	SSL (MIM)	Cls.	SSL (CL)	SSL (MIM)	Gen.	Gen.	Det.	Seg.
EMA	0.99	0.999	0.9	0.9999	0.999	0.9999	0.99996	0.999	0.9999	0.9999	0.9999	0.9999
SEMA	0.99	0.999	0.999	0.999	0.999	0.999	0.9999	0.999	0.9999	0.9999	0.999	0.999

Table A2: Momentum coefficient α in EMA and SEMA for regression (Reg.), video prediction (VP), language processing (LP), text classification (Cls.), and language modeling (LM) tasks.

Dataset	RCFMNIST	AgeDB	IMDB-WIKI	MMNIST	Penn TreeBank	Yelp Review	WikiText-103
Task	Reg.	Reg.	Reg.	VP	LP	Cls.	LM
EMA	0.999	0.999	0.999	0.999	0.9999	0.9999	0.9999
SEMA	0.999	0.999	0.999	0.999	0.999	0.999	0.999

Table A3: Ingredients and hyper-parameters used for ImageNet-1K training settings with various optimizers. Note that the settings of PyTorch (Simonyan & Zisserman, 2014), RSB A2 and A3 (Wightman et al., 2021), and LARS (Ginsburg et al., 2018) take ResNet-50 as the examples, DeiT (Touvron et al., 2021) and Adan (Xie et al., 2023) settings take DeiT-S as the example, and the ConvNeXt (Liu et al., 2022d) setting is a variant of the DeiT setting for ConvNeXt and Swin Transformer (Liu et al., 2021) architectures.

Procedure	PyTorch	DeiT	ConvNeXt	RSB A2	RSB A3	Adan	LARS
Train Resolution	224	224	224	224	160	224	160
Test Resolution	224	224	224	224	224	224	224
Test crop ratio	0.875	0.875	0.875	0.95	0.95	0.85	0.95
Epochs	100	300	300	300	100	150	100
Batch size	256	1024	4096	2048	2048	2048	2048
Optimizer	SGD	AdamW	AdamW	LAMB	LAMB	Adan	LARS
Learning rate	0.1	1×10^{-3}	4×10^{-3}	5×10^{-3}	8×10^{-3}	1.6×10^{-2}	8×10^{-3}
Optimizer Momentum	0.9	0.9, 0.999	0.9, 0.999	0.9, 0.999	0.9, 0.999	0.98, 0.92, 0.99	0.9
LR decay	Cosine	Cosine	Cosine	Cosine	Cosine	Cosine	Cosine
Weight decay	10^{-4}	0.05	0.05	0.02	0.02	0.02	0.02
Warmup epochs	\times	5	20	5	5	60	5
Label smoothing ϵ	\times	0.1	0.1	\times	\times	0.1	\times
Dropout	\times	\times	\times	\times	\times	\times	\times
Stochastic Depth	\times	0.1	0.1	0.05	\times	0.1	\times
Repeated Augmentation	\times	\checkmark	\checkmark	\checkmark	\times	\times	\times
Gradient Clip.	\times	5.0	\times	\times	\times	5.0	\times
Horizontal flip	\checkmark	\checkmark	\checkmark	\checkmark	\checkmark	\checkmark	\checkmark
RandomResizedCrop	\checkmark	\checkmark	\checkmark	\checkmark	\checkmark	\checkmark	\checkmark
Rand Augment	\times	9/0.5	9/0.5	7/0.5	6/0.5	7/0.5	6/0.5
Auto Augment	\times	\times	\times	\times	\times	\times	\times
Mixup α	\times	0.8	0.8	0.1	0.1	0.8	0.1
Cutmix α	\times	1.0	1.0	1.0	1.0	1.0	1.0
Erasing probability	\times	0.25	0.25	\times	\times	0.25	\times
ColorJitter	\times	\times	\times	\times	\times	\times	\times
EMA	\times	\checkmark	\checkmark	\times	\times	\times	\times
CE loss	\checkmark	\checkmark	\checkmark	\times	\times	\checkmark	\times
BCE loss	\times	\times	\times	\checkmark	\checkmark	\times	\checkmark

23×23 with a standard deviation uniformly sampled in $[0.1, 2.0]$. We use the same setting on CIFAR-100 and STL-10, where the input resolution of CIFAR-100 is resized to 224^2 . The pre-training epoch on CIFAR-100 and STL-10 is 1000, while it is set to the official setup on ImageNet-1K, as shown in Table 5. As for the evaluation protocol, we follow

MoCo.V2 and MoCo.V3 to conduct linear probing upon pre-trained representations. Note that MoCo.V2, BYOL, and MoCo.V3 require EMA with the momentum of 0.999, 0.99996, and 0.99996 as the teacher model, while SimCLR and Barlow Twins do not need WA methods by default.

Table A4: Ingredients and hyper-parameters used for pre-training on ImageNet-1K various SSL methods. Note that CL methods require complex augmentations proposed in SimCLR (SimCLR Aug.) and evaluated by Linear probing, while MIM methods use fine-tuning (FT) protocols.

Configuration	SimCLR	MoCo.V2	BYOL	Barlow Twins	MoCo.V3	MAE	SimMIM/A ² MIM
Pre-training resolution	224 × 224	224 × 224	224 × 224	224 × 224	224 × 224	224 × 224	224 × 224
Encoder	ResNet	ResNet	ResNet	ResNet	ViT	ViT	ViT
Augmentations	SimCLR Aug.	SimCLR Aug.	SimCLR Aug.	SimCLR Aug.	SimCLR Aug.	RandomResizedCrop	RandomResizedCrop
Mask patch size	×	×	×	×	×	16 × 16	32 × 32
Mask ratio	×	×	×	×	×	75%	60%
Projector / Decoder	2-MLP	2-MLP	2-MLP	3-MLP	2-MLP	ViT Decoder	FC
Optimizer	SGD	LARS	LARS	LARS	AdamW	AdamW	AdamW
Base learning rate	4.8	3×10^{-2}	4.8	1.6	2.4×10^{-3}	1.2×10^{-3}	4×10^{-4}
Weight decay	1×10^{-4}	1×10^{-6}	1×10^{-6}	1×10^{-6}	0.1	0.05	0.05
Optimizer momentum	0.9	0.9	0.9	0.9	0.9, 0.95	0.9, 0.999	0.9, 0.999
Batch size	4096	256	4096	2048	4096	2048	2048
Learning rate schedule	Cosine	Cosine	Cosine	Cosine	Cosine	Cosine	Step / Cosine
Warmup epochs	10	×	10	10	40	10	10
Gradient Clipping	×	×	×	×	max norm= 5	max norm= 5	max norm= 5
Evaluation	Linear	Linear	Linear	Linear	Linear	FT	FT

Masked Image Modeling. As for generative pre-training with MIM methods, we choose SimMIM (Xie et al., 2022) and A²MIM (Li et al., 2023a) to perform pre-training and fine-tuning with ViT (Dosovitskiy et al., 2020) on CIFAR-100, STL-10, and ImageNet-1K. Similarly, two MIM methods utilize their official pre-training setting on ImageNet-1K for three datasets, as shown in Table A4. CIFAR-100 and STL-10 use 224² and 96² resolutions to pre-train DeiT-S for 1000 epochs while ImageNet-1K uses 224² resolutions to pre-training ViT-B for 800 epochs. The fine-tuning evaluation protocols are also adopted as their original recipes, fine-tuning 100 epochs with a layer decay ratio of 0.65 with the AdamW optimizer. Note that both the MIM methods do not require WA techniques during pre-training.

B.3. Object Detection and Instance Segmentation

Following Swin Transformers (Liu et al., 2021; Li et al., 2024b), we evaluate objection detection and instance segmentation tasks on COCO (Lin et al., 2014) dataset, which include 118K training images (*train2017*) and 5K validation images (*val2017*). Experiments of COCO detection and segmentations are implemented on MMDetection (Chen et al., 2019) codebase and run on 4 Tesla V100 GPUs.

Fine-tuning. Taking ImageNet pre-trained ResNet-50 and Swin-T as the backbone encoders, we adopt RetinaNet (Lin et al., 2017), Mask R-CNN (He et al., 2017), and Cascade Mask R-CNN (Cai & Vasconcelos, 2019) as the standard detectors. As for ResNet-50, we employ the SGD optimizer for training 2× (24 epochs) and 3× (36 epochs) settings with a basic learning rate of 2×10^{-2} , a batch size of 16, and a fixed step learning rate scheduler. Since MMDetection uses repeat augmentation for Cascade Mask R-CNN, its training 1× and 3× with multi-scale (MS) resolution and advanced data augmentations equals training 3× and 9×,

which can investigate the regularization capacities of WA techniques. As for Swin-T, we employ AdamW (Loshchilov & Hutter, 2019) optimizer for training 1× schedulers (12 epochs) with a basic learning rate of 1×10^{-4} and a batch size of 16. During training, the shorter side of training images is resized to 800 pixels, and the longer side is resized to not more than 1333 pixels. We calculate the FLOPs of compared models at 800×1280 resolutions. The momentum of EMA and SEMA is 0.9999 and 0.999.

Training from Scratch. For the YoloX (Ge et al., 2021) detector, we follow its training settings with randomly initialized YoloX-S encoders (the modified version of CSPDarkNet). The detector is trained 300 epochs by SGD optimizer with a basic learning rate of 1×10^{-2} , a batch size of 64, and a cosine annealing scheduler. During training, input images are resized to 640 × 640 resolutions and applied complex augmentations like Mosaic and Mixup (Zhang et al., 2018; Liu et al., 2022c). The momentum of EMA and SEMA is 0.9999 and 0.999.

B.4. Image Generation

Following DDPM (Ho et al., 2020), we evaluated image generation tasks based on CIFAR-10 (Krizhevsky et al., 2009), which includes 5K training images and 1K testing images (a total of 6K images). The training was conducted with a batch size of 128, performing 1000 training steps per second and using a learning rate of 2×10^{-4} . The DDPM-torch codebase was utilized to implement the DDPM image generation experiments executed on 4 Tesla V100 GPUs. Similarly, for the CelebA dataset (Liu et al., 2015), which includes 162,770 training images, 19,867 validation images, and 19,962 testing images (a total of 202,599 images), image generation tasks were performed with a batch size of 128. The training was conducted with 1000 training steps

per second, and the learning rate was set to $2e-5$. The `ddpm-torch`¹ codebase was employed for implementing the DDPM image generation experiments, which were executed on 4 Tesla V100 GPUs. For the two datasets, the models utilized EMA and SEMA, with an ema decay factor set to the default value of 0.9999. The total number of epochs required for training the CIFAR-10 model is 2000 and 600 CelebA, optimized by Adam (Kingma & Ba, 2014) and a batch size of 128. In the final experiment, the model was trained once, and checkpoints were saved at regular intervals (every 50 epochs for CIFAR-10 and every 20 epochs for CelebA). Then, using 4 GPUs and the DDIM (Song et al., 2021) sampler, 50,000 samples were generated in parallel for each checkpoint. Finally, the FID score (Simonyan & Zisserman, 2014) was computed using the codebase to evaluate the 50,000 generated samples and record the results.

B.5. Video Prediction

Following SimVP (Gao et al., 2022) and OpenSTL (Tan et al., 2023), we verify WA methods with video prediction methods on Moving MNIST (Srivastava et al., 2015). We evaluate various Metaformer architectures (Yu et al., 2022) and MogaNet with video prediction tasks on Moving MNIST (MMNIST) (Lin et al., 2014) based on SimVP (Gao et al., 2022). Notice that the hidden translator of SimVP is a 2D network module to learn spatiotemporal representation, which any 2D architecture can replace. Therefore, we can benchmark various architectures based on the SimVP framework. In MMNIST (Srivastava et al., 2015), each video is randomly generated with 20 frames containing two digits in 64×64 resolutions, and the model takes 10 frames as the input to predict the next 10 frames. Video predictions are evaluated by Mean Square Error (MSE), Mean Absolute Error (MAE), and Structural Similarity Index (SSIM). All models are trained on MMNIST from scratch for 200 or 2000 epochs with Adam optimizer, a batch size of 16, a OneCycle learning rate scheduler, an initial learning rate selected in $\{1 \times 10^{-2}, 5 \times 10^{-3}, 1 \times 10^{-3}, 5 \times 10^{-4}\}$. Experiments of video prediction are implemented on OpenSTL codebase (Tan et al., 2023) and run on a single NVIDIA Tesla V100 GPU.

B.6. Visual Attribute Regression

As for regression tasks, we conducted age regression experiments on two datasets: IMDB-WIKI (Rothe et al., 2018) and AgeDB (Moschoglou et al., 2017). AgeDB comprises images of various celebrities, encompassing actors, writers, scientists, and politicians, with annotations for identity, age, and gender attributes. The IMDB-WIKI dataset comprises approximately 167,562 face images, each associated with an age and gender label. The age range of the two datasets

is from 1 to 101. In age regression tasks, our objective is to extract human features that enable the model to predict age as a continuous real value. Meanwhile, we also consider a rotation angle regression task on RCF-MNIST (Yao et al., 2022) dataset, which incorporates a more complex background inspired by CIFAR-10 to resemble natural images closely. This task allows the model to regress the rotation angle of the foreground object. We adopted the same experimental settings as described in SemiReward (Li et al., 2024a) and C-Mixup (Yao et al., 2022). In particular, we used ConvNeXt-T, ResNet-18, and ResNet-50 as backbone models, in addition to using a variety of methods for comparison. The input resolutions were set to 224^2 for AgeDB and IMDB-WIKI and 32^2 for RCF-MNIST. Models are optimized with ℓ_1 loss and the AdamW optimizer for 400 or 800 epochs for AgeDB/IMDB-WIKI or RCF-MNIST datasets. MAE and RMSE are used as evaluation metrics.

B.7. Language Processing

Penn TreeBank with LSTM. Following Adabief (Zhuang et al., 2020), the language processing experiment with LSTM (Ma et al., 2015) is conducted with Penn TreeBank dataset (Marcus et al., 1993) (with 887,521 training tokens, 70,390 validation tokens, 78,669 test tokens, vocab of 10,000, and 4.8% OoV) on LSTM with Adan as the baseline, utilizing its default weight decay (0.02) and *betas* ($\beta_1 = 0.02$, $\beta_2 = 0.08$, $\beta_3 = 0.01$), and a learning rate of 0.01. We applied EMA and SEMA for comparison, and momentum defaults to 0.999 and 0.9999. We fully adhere to the experimental settings in Adabief and use its codebase, applying the default settings for all other hyperparameters provided by Adabief (weight decay= $1.2e-6$, eps= $1e-8$, batch size=80, a total of 8000 epochs for single training). We use Perplexity as the primary evaluation metric for observing the training situation of SEMA.

Text Classification with Yelp Review. Second, for the Yelp review task in USB (Wang et al., 2022), we use the pre-trained BERT (Devlin et al., 2018) and experiment on the Yelp review dataset (Yel). The dataset contains a large number of user reviews and is made up of five classes (scores), each containing 130,000 training samples and 10,000 test samples. For BERT under USB, we adopt the Adam optimizer with a weight decay of $1e-4$, a learning rate of $5e-5$, and a layer decay ratio of 0.75, and the Momentum default values for SEMA and EMA are the same as before. We also fully adhere to and utilize its fully-supervised setting.

Language Modeling with WikiText-103. We also conducted language modeling experiments on WikiText-103 (Ott et al., 2019) (with 103,227,021 training tokens, 217,646 validation tokens, 245,569 test tokens, and vocabulary of 267,735). In the comprehensive experimental, the

¹<https://github.com/tqch/ddpm-torch/>

sequence length was set to 512, and the experiment settings followed the specifications of fairseq (weight decay was 0.01, using the Adam optimizer, and learning rate of 0.0005). The default Momentum values for EMA and SEMA were maintained for training and evaluation, and the final comparison was based on Perplexity.

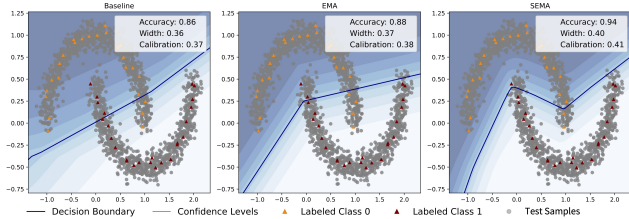


Figure A1: Illustration of the baseline, EMA, and SEMA on Two Moons Dataset with 50 labeled samples (triangle red/yellow points) with others as testing samples (grey points) in training a 2-layer MLP classifier. We evaluate the performance by computing top-1 accuracy, decision boundary width, and prediction calibration.

C. Empirical Experiments

Loss Landscape. The 1D linear interpolation method (Goodfellow et al., 2015) assesses the loss value along the direction between two minimizers of the same network loss function (Li et al., 2017). We visualize the 1d loss landscape 2b of the model guided by SEMA, using CNNs and Vits as backbones and SEMA showed sharper precision and loss lines compared to the baseline model, EMA and SAM, indicating better performance. To plot the 2d loss landscape 4, we select two random directions and normalize them in the same way as in the 1D plot. By observing the different trajectories of the two models from the same initial point and their final positions relative to the local minimum, we can effectively compare them. SEMA ultimately converges rapidly to the position closest to the local minimum, while EMA remains trapped in a flat local basin. This effectively demonstrates that SEMA can converge faster and more efficiently.

Decision Boundary. We trained a 2-layer MLP classifier using the SGD optimizer with a fixed learning rate of 0.01 on a binary classification dataset from sklearn (Pedregosa et al., 2011). The dataset consisted of circular and moon-shaped data points, with 50 labeled samples represented by red or yellow triangles and the remaining samples as grey circles for testing purposes. We compared the performance of the baseline model, EMA, and SEMA. When plotting the decision boundaries (He et al., 2018), we used smooth, solid lines to represent the boundaries (3, A1). Each algorithm was distinguished by using distinct colors. The transition of the test samples from blue to grey represented the confidence of the network predictions. Furthermore,

SEMA can be further compared and evaluated according to the evaluation indicators. One is accuracy, that is, the ability to divide test samples; the other is Calibration, the closer the decision boundary, the less trustworthy it will be, and the lower the classification accuracy will be; the third is the width of the decision boundary, the wider the decision boundary, the more robust it will be. According to the intuitive comparison, SEMA can achieve the most accurate classification and is superior to EMA and the baseline model in all evaluation indicators, effectively indicating that SEMA has higher performance and robustness.

D. Extensive Related Work

D.1. Optimizers

With the advent of BP (Rumelhart et al., 1986) and SGD (Sinha & Griscik, 1971) with mini-batch training (Bishop, 2006), optimizers have become an indispensable component in the training process of DNNs. Various mainstream optimizers leverage momentum techniques (Sutskever et al., 2013) to accumulate gradient statistics, which are crucial for improving the convergence and performance of DNNs. In addition, adaptive learning rates such as those found in Adam variants (Kingma & Ba, 2014; Liu et al., 2020) and acceleration schemes (Kobayashi, 2020) have been used to enhance these capabilities further. SAM method (Foret et al., 2021) works by searching for a flatter region where the training losses in the estimated neighborhood are minimized through min-max optimizations. Its variants aim to improve training efficiency from various perspectives, such as gradient decomposition (Zhuang et al., 2022) and training costs (Du et al., 2021; 2022) (Liu et al., 2022a). To expedite training, large-batch optimizers like LARS (Ginsburg et al., 2018) for SGD and LAMB (You et al., 2020) for AdamW (Loshchilov & Hutter, 2019) have been proposed. These optimizers adaptively adjust the learning rate based on the gradient norm to facilitate faster training. Adan (Xie et al., 2023) introduces Nesterov descending to AdamW, bringing improvements across popular computer vision and natural language processing applications. Moreover, a new line of research has proposed plug-and-play optimizers such as Lookahead (Zhang et al., 2019; Zhou et al., 2021) and Ranger (Wright, 2019). These optimizers can be combined with existing inner-loop optimizers (Zhou et al., 2021), acting as the outer-loop optimization to improve generalization and performance while allowing for faster convergence.

D.2. Weight Averaging

In stark contrast to gradient momentum updates in optimizers, weight averaging (WA) techniques such as SWA (Izmailov et al., 2018) and EMA (Polyak & Juditsky, 1992) are commonly employed during DNN training to enhance

model performance further. Test-time WA strategies, including SWA variants (Maddox et al., 2019) and FGE variants (Guo et al., 2023; Garipov et al., 2018), employ the heuristic of ensembling different models from multiple iterations (Granzio et al., 2021) to achieve flat local minima and thereby improve generalization capabilities. Notably, TWA (Li et al., 2023b) has improved upon SWA by implementing a trainable ensemble. Another important weighted averaging technique targeted explicitly at large models is Model Soup (Wortsman et al., 2022), which leverages solutions obtained from different fine-tuning configurations. Greedy Soup improves model performance by sequentially greedily adding weights. When applied during the training phase, the EMA update can significantly improve the performance and stability of existing optimizers across various domains. EMA is an integral part of certain learning paradigms, including popular semi-supervised learning methods such as FixMatch variants (Sohn et al., 2020), and self-supervised learning (SSL) methods like MoCo variants (He et al., 2020; Chen et al., 2021), and BYOL variants (Grill et al., 2020). These methods utilize a self-teaching framework, where the teacher model parameters are the EMA version of student model parameters. In the field of reinforcement learning, A3C (Mnih et al., 2016) employs EMA to update policy parameters, thereby stabilizing the training process. Furthermore, in generative models like diffusion (Karras et al., 2023), EMA significantly contributes to the stability and output distribution. Recent efforts such as LAWA (Kaddour, 2022) and PSWA (Guo et al., 2022) have explored the application of EMA or SWA directly during the training process. However, they found that while using WA during training can accelerate convergence, it does not necessarily guarantee final performance gains. SASAM (Kaddour et al., 2022) combines the complementary merits of SWA and SAM to achieve local flatness better. Despite these developments, the universal applicability and ease of migration of these WA techniques make them a crucial focus for ongoing innovation. This paper aims to improve upon EMA by harnessing the historical exploration of a single configuration and prioritizing training efficiency to achieve faster convergence.

D.3. Regularizations

In addition to the optimizers, various regularization techniques have been proposed to enhance the generalization and performance of DNNs. Techniques such as weight decay (Andriushchenko et al., 2023) and dropout variants (Srivastava et al., 2014; Huang et al., 2016) are designed to control the complexity of the network parameters and prevent overfitting, which have been effective in improving model generalization. These techniques, including EMA, fall under network parameter regularizations. Specifically, the EMA has shown to effectively regularize Transformer (De-

vlin et al., 2018; Touvron et al., 2021) training across both computer vision and natural language processing scenarios (Liu et al., 2022d; Wightman et al., 2021). Another set of regularization techniques aims to improve generalizations by modifying the data distributions. These include label regularizers (Szegedy et al., 2016) and data augmentations (DeVries & Taylor, 2017). Data-dependent augmentations like Mixup variants (Zhang et al., 2018; Yun et al., 2019; Liu et al., 2022c) and data-independent methods such as RandAugment variants (Cubuk et al., 2019; 2020) increase data capacities and diversities. These methods have achieved significant performance gains while introducing negligible additional computational overhead. Most regularization methods, including our proposed SEMA, provide ‘free lunch’ solutions. They can effectively improve performance as a pluggable module without incurring extra costs. In particular, SEMA enhances generalization abilities as a plug-and-play step for various application scenarios.